arXiv:2506.09312v1 [cs.CR] 11 Jun 2025

What is the Cost of Differential Privacy for Deep Learning-Based Trajectory Generation?

Erik Buchholz
University of New South Wales
CSIRO's Data61, Cyber Security CRC
Sydney, NSW, Australia
e.buchholz@unsw.edu.au

Natasha Fernandes
Macquarie University
Sydney, NSW, Australia
natasha.fernandes@mq.edu.au

David D. Nguyen
CSIRO's Data61
Sydney, NSW, Australia
david.nguyen@data61.csiro.au

Alsharif Abuadbba
CSIRO's Data61, Cyber Security CRC
Sydney, NSW, Australia
sharif.abuadbba@data61.csiro.au

Surya Nepal
CSIRO's Data61, Cyber Security CRC
Sydney, NSW, Australia
surya.nepal@data61.csiro.au

Salil S. Kanhere
University of New South Wales
Sydney, NSW, Australia
salil.kanhere@unsw.edu.au

***Abstract*—While location trajectories offer valuable insights, they also reveal sensitive personal information. Differential Privacy (DP) offers formal protection, but achieving a favourable utility-privacy trade-off remains challenging. Recent works explore deep learning-based generative models to produce synthetic trajectories. However, current models lack formal privacy guarantees and rely on conditional information derived from real data during generation. This work investigates the utility cost of enforcing DP in such models, addressing three research questions across two datasets and eleven utility metrics. (1) We evaluate how DP-SGD, the standard DP training method for deep learning, affects the utility of state-of-the-art generative models. (2) Since DP-SGD is limited to unconditional models, we propose a novel DP mechanism for conditional generation that provides formal guarantees and assess its impact on utility. (3) We analyse how model types – Diffusion, VAE, and GAN – affect the utility-privacy trade-off. Our results show that DP-SGD significantly impacts performance, although some utility remains if the datasets is sufficiently large. The proposed DP mechanism improves training stability, particularly when combined with DP-SGD, for unstable models such as GANs and on smaller datasets. Diffusion models yield the best utility without guarantees, but with DP-SGD, GANs perform best, indicating that the best non-private model is not necessarily optimal when targeting formal guarantees. In conclusion, DP trajectory generation remains a challenging task, and formal guarantees are currently only feasible with large datasets and in constrained use cases.**

1. Introduction

Various services, such as navigation (Google Maps), transport (Uber), and social gaming (Pokémon Go), collect vast amounts of location data. While the collected location trajectories are valuable for various applications, from urban planning to disease spread analysis, they also contain sensitive information about individuals [1]. For example, four locations suffice to identify 95 % of users from phone connection data [2], and taxi drivers' break times can reveal whether they are practising Muslims [3]. Accordingly, a large body of research is dedicated to the privacy of trajectory data [1, 4, 5, 6]. Due to their formal guarantees, significant research has focused on mechanisms with Differential Privacy (DP) [7]. Yet, the challenging utility-privacy trade-off, vulnerability to reconstruction attacks [8, 9], and other limitations hinder their real-world applicability [6, 7].

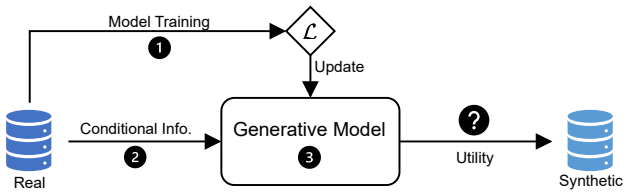

Figure 1. Research questions: How do (1) DP-SGD, (2) DP conditional information, and (3) model architectures affect the utility and privacy trade-off of trajectory generation?

To address the limitations of releasing a protected dataset, Liu et al. [10] suggested generating synthetic data that can be released instead of the private dataset. Subsequently, various deep learning-based generative models for trajectory data have been developed. Many of these approaches yield utility that substantially surpasses the traditional publication approaches. Yet, Buchholz et al. [6] find that no existing deep learning model provides formal privacy guarantees.

As illustrated in Figure 1, private information can flow over two paths from the real dataset into the synthetic data. First, during training, the model updates its parameters to learn the real data distribution. While the specifics depend on the model and loss function, the parameters must encode some real data information to generate meaningful results. Second, some models use input derived from the

real dataset, referred to as *conditional information*, which guides generation [11, 12]. This input can represent derived attributes [11], such as average speed or start location, or entire trajectories [12]. Although few unconditional models exist [11], most SOTA generative trajectory models rely on such conditional information to yield meaningful utility [6].

Due to the potential of deep learning-based generative trajectory models, this study addresses the overarching research question: *What is the (utility) cost of formal privacy guarantees for deep learning-based trajectory generation*? Since DP serves as the current de facto standard for privacy, our analysis focuses on this technique to ensure formal guarantees. While non-Deep Learning (DL) approaches for DP trajectory generation exist, these have already been thoroughly reviewed by multiple existing studies [6, 7, 13, 14]. Therefore, this study explicitly focuses on deep learning-based trajectory generation which has not been comprehensively evaluated regarding formal privacy guarantees before. Following Figure 1, the study seeks to answer the research question by examining the impact of three factors:

① First, we assess the impact of formal guarantees with respect to (w.r.t.) the training data on utility. As Differentially Private Stochastic Gradient Descent (DP-SGD) is the most widely used method for providing DP guarantees w.r.t. a DL model's training data [15], we pose the following question:

RQ1. *How does DP-SGD affect the generated trajectories' utility?*

We find that using DP-SGD with a realistic privacy parameter ($\varepsilon = 10$) leads to a significant utility loss, which is restrictive for most practical applications, especially on smaller datasets. However, comparison with the SOTA baseline PrivTrace [16] shows that this loss is in line with non-DL approaches.

② For unconditional models without additional input, DP-SGD ensures formal privacy guarantees w.r.t. the generated data. However, most SOTA models perform significantly better with conditional information [11, 12, 17]. Directly using cond. info. during generation poses a critical privacy risk, as even statistical data can leak private information and violate DP guarantees. For instance, LSTM-TrajGAN has been shown to converge towards an identity function when overtrained [6]. However, to the best of our knowledge, no trajectory-level DP approach for conditional information has been proposed, leading to the second research question:

RQ2. *How can we use conditional information with differential privacy guarantees?*

To tackle this, we introduce a novel DP embedding for conditional information, combining compression and clipping with a DP mechanism and prove its guarantees formally. This DP cond. info. can enhance utility and stabilise training while providing guarantees in some settings, especially for Generative Adversarial Networks (GANs), combined with DP-SGD, and on smaller datasets.

③ While diffusion models consistently outperform other approaches for trajectory generation without privacy guarantees [11, 17, 18], other architectures, such as GANs and Variational Autoencoders (VAEs), can be adapted with minimal modifications. The reduced training time of or the distinct structure of GANs may influence the utility-privacy trade-off under formal guarantees, motivating the third research question:

RQ3. *Are certain model types better suited for formal privacy guarantees than others?*

Specifically, we aim to determine whether the best-performing non-DP model also remains the best-performing DP model or if trends shift when applying formal guarantees. To address this, we compare a diffusion model, a VAE, and a GAN, all derived from a similar UNet architecture. Aligning with the findings of related work [11], the conditional diffusion model yields the best performance without formal guarantees, although the VAE achieves competitive results especially on the smaller dataset. However, when considering full formal guarantees, the VAE cannot compare with the diffusion model while the GAN performs even superior.

Contributions. To provide a comprehensive evaluation, we follow the framework of Buchholz et al. [6] and evaluate on two public datasets, namely Porto [19] and GeoLife [20], across eleven metrics, covering all four types of trajectory utility [6]. This study contributes to trajectory privacy by:

1. Quantifying the *utility cost of DP-SGD* on SOTA trajectory generation models.
2. Proposing a method to utilise *conditional information without violating differential privacy*, proving its privacy guarantees, and evaluating its impact on utility.
3. Comparing the utility-privacy trade-off of *three model types*: Diffusion, VAE, and GAN.
4. Conducting a comprehensive evaluation using *eleven metrics* and *two datasets* including one SOTA non-DL baseline [16].
5. Publishing all code and data to support further research[1].

2. Background

This section outlines relevant background knowledge. It defines the trajectory dataset (Section 2.1), introduces differential privacy (Section 2.2), and reviews generative models (Section 2.3) and DP-SGD (Section 2.4).

2.1. Trajectory

A trajectory dataset is a set of n trajectories $D = \{T_1, T_2, \ldots, T_n\}$. Each trajectory T_i represents an ordered sequence of points:

$$T_i = \left(p_1^{(i)}, p_2^{(i)}, \ldots, p_L^{(i)}\right)$$

where L is the length of the trajectory. In this work, we assume that each point $p_j^{(i)}$ consists of at least two location coordinates, typically geographical coordinates such as latitude and longitude: $p_j^{(i)} = (lat, lon)$. Trajectories may include temporal or semantic context [21], but this work focuses solely on location information.

1. https://github.com/erik-buchholz/CostOfTrajectoryPrivacy

2.2. Differential Privacy

Privacy notions are commonly classified as *syntactic* or *semantic* [22]. *Differential Privacy (DP)* [23] represents the primary semantic notion for protecting personal data [22, 24]. Differential Privacy ensures that the inclusion or exclusion of a single user's data does not significantly affect the output, offering *plausible deniability* regarding participation in the dataset. Formally, a mechanism satisfies (ε, δ)-DP if [23]:

Definition 1 (Differential Privacy [23])**.** *A mechanism $\mathcal{K}$ provides (ε, δ)-differential privacy if for all adjacent datasets D_1 and D_2 ($Adj(D_1, D_2)$), and all $S \subseteq Range(\mathcal{K})$:*

$$\mathbb{P}\left[\mathcal{K}(D_1) \in S\right] \leq e^{\varepsilon} \times \mathbb{P}\left[\mathcal{K}(D_2) \in S\right] + \delta \tag{1}$$

The main privacy parameters in differential privacy are ε and δ. Typical values for ε range from 0.01 to 10, with $\varepsilon \leq 1$ considered strong and $\varepsilon \leq 10$ realistic [25]. In DL, larger ε values are often used in practice, as they may still offer empirical protection [15]. Best practice is to set $\delta \ll 1/n$, e.g., $\delta = 1/n^{1.1}$, where n is the dataset size [15].

Differential Privacy requires defining when two datasets are *neighbouring* (Adj). The two most common adjacency relations are *add-or-remove* and *replace-one* (or *substitution*) [15]. Add-or-remove treats datasets as adjacent if one can be obtained from the other by adding or removing a single record. Replace-one assumes one record is replaced, keeping the dataset size fixed. The replace-one relation is approximately twice as strong, as it combines both adding and removing a record [15] (e.g., $\varepsilon = 2$ under replace-one is roughly as strong as $\varepsilon = 1$ under add-or-remove). While add-or-remove is more common, replace-one enables the analysis of mechanisms requiring a fixed number of records. Moreover, the Unit of Privacy (UoP) [6, 15] defines what constitutes a single record. While standard DP aims for *user-level* privacy, we adopt the *trajectory-level* notion, treating each trajectory as a record [6]. This is common in DL, where guarantees are typically applied per training sample, reducing utility loss at the cost of weaker privacy guarantees [15].

Additionally, DP provides *composition theorems* that enable combining multiple mechanisms while preserving formal guarantees. For example, it is invariant to post-processing and supports both sequential and parallel composition [23].

DP can be achieved through various mechanisms:

Laplace Mechanism. The *Laplace mechanism* [23] is commonly used for continuous values. It adds i.i.d. noise drawn from $\mathcal{L}(\Delta_1 f/\varepsilon)$ to each component of a function $f(X)$, where $\Delta_1 f$ is the l_1 sensitivity, i.e., the maximum change in f between any two adjacent datasets. This yields a mechanism that satisfies ε-DP.

Gaussian Mechanism. The Gaussian mechanism adds noise based on the l_2-sensitivity $\Delta_2 f$, making it preferable for high-dimensional functions f. It samples from a normal distribution $\mathcal{N}(0, \sigma^2)$, where $\sigma = {}^{\Delta_2 f}/_{\varepsilon} \cdot \sqrt{2\ln(1.25/\delta)}$ ensures (ε, δ)-differential privacy for $\varepsilon, \delta \in (0, 1)$ [23]. Balle and Wang [26] propose the analytical Gaussian mechanism, which applies to any $\varepsilon > 0$ and provides tighter bounds.

VMF Mechanism. The *Von Mises-Fisher Distribution (VMF)* mechanism [27] provides DP guarantees by sampling from a VMF distribution, defined over unit vectors $v \in \mathbb{R}^d$ with $\|v\|_2 = 1$. Its PDF is

$$\mathcal{V}(\kappa, \mu)(x) = C_d(\kappa) e^{\kappa \mu^T x} \tag{2}$$

where $\kappa > 0$ is the concentration parameter, μ is the mean direction, and $C_d(\kappa)$ is a normalisation constant. The mechanism satisfies $(\varepsilon, 0)$-DP when $\kappa = {}^{\varepsilon}/_{\Delta_2 f}$.

2.3. Generative Models

Generative models for sequential data [28], such as trajectories, address limited data availability and enable synthetic data generation for sensitive domains.

Autoencoders (AEs) [29] consist of an encoder that maps inputs to a lower-dimensional latent representation and a decoder that reconstructs the original input. The latent bottleneck forces the outputs to differ, while the most important information is preserved.

Variational Autoencoders (VAEs) [30] extend AEs by encoding inputs into a latent distribution with mean μ and standard deviation σ. The decoder samples from this distribution to reconstruct the input. The loss combines a reconstruction loss and the KL divergence, encouraging the latent space to converges towards $\mathcal{N}(0, 1)$. For reconstruction, the decoder samples from the distribution defined by the encoder, while for generation, it samples from the standard normal distribution $\mathcal{N}(0, 1)$ generating new unseen samples.

Generative Adversarial Networks (GANs) [31] consist of a generator G and a discriminator D. The generator G transforms input noise $z \sim p_z$ into samples resembling real data, while the discriminator D evaluates whether a sample is real or generated. The generator and discriminator train iteratively until G produces samples that are indistinguishable from real data (for the discriminator).

Diffusion Models [32] generate data by denoising Gaussian noise through a learned reverse diffusion process. Starting from $\hat{x}_T \sim \mathcal{N}(0, I)$, the model iteratively predicts and removes noise to recover $\hat{x}_0$. During training, noise is incrementally added to real data x_0 in the *forward diffusion process*, effectively converting the sample into Gaussian noise. UNet [33] architectures are commonly used. Diffusion models produce high-quality outputs with stable training but are slower to sample compared to GANs or VAEs.

2.4. Differentially Private SGD

DL models are often trained on sensitive data containing personal or proprietary information. MIAs [34] have shown that such models can leak training data, even if the data itself is not published. To mitigate this, DP has been applied to DL [15, 35]. We refer to Ponomareva et al. [15] for a comprehensive overview and focus here on *DP-SGD* [35], the most widely used method to achieve DP in DL. The core idea behind DP-SGD is the addition of Gaussian noise to the gradients, which are used to update the weights of the model. The required noise level depends on the sensitivity Δf of the mechanism (ref. Section 2.2), which in DL corresponds to the influence of a single training sample.

Since gradient norms are generally unbounded, DP-SGD first clips per-sample gradients to a norm bound C. Second, Gaussian noise is added to the gradients based on this clipping norm C and a noise multiplier σ. A privacy accountant tracks the accumulated privacy loss during training, yielding a final (ε, δ)-DP guarantee. The noise multiplier can be estimated in advance to target a specific privacy budget.

3. Threat Model

As shown in Figure 1, synthetic data generation can leak private information during *training* of the generative model (①) or *generation* of synthetic data (②). Therefore, we distinguish four threat models based on the guarantees during training and generation. We consider a private dataset D, partitioned into disjoint training (D_{train}) and test (D_{test}) sets, where D_{test} provides conditional information for generation.

This work targets trajectory-level guarantees [6], where each sample corresponds to a single trajectory. While user-level guarantees are stronger, sample-level guarantees are more common in deep learning [15] and offer a reasonable trade-off between utility and privacy (ref. Section 2.2).

Ⓐ **No Guarantees.** At this level, no formal privacy guarantees are provided. Privacy relies solely on the synthetic data's inherent properties and assumes that used conditional information does not leak sensitive details. For instance, using statistical features as done by DiffTraj [11], may be acceptable in low-risk scenarios. Most SOTA models [6, 11, 12] operate in this setting without formal guarantees.

Ⓑ **Training-level Guarantees.** Guarantees apply only to the training data D_{train}, offering protection against attacks such as MIA [34]. This setting is relevant when conditional information is non-sensitive or the risk of leakage during generation is low. For example, a conditional model could use synthetic or public conditional data.

Ⓒ **Generation Guarantees.** This level ensures privacy only during generation w.r.t. the test set D_{test}. Unconditional models inherently satisfy this, as they use no input during generation, yielding 0-DP w.r.t. D_{test}. This setting is relevant when model or output leakage is unlikely, or if training uses public data and generation uses private data.

Ⓓ **Full Guarantees.** This level combines Ⓑ and Ⓒ, offering formal guarantees for both the training data and any cond. info. used during generation. While providing the strongest protection, it may lead to significant utility loss.

4. Related Work

The potential value of trajectory data for various applications has driven extensive research on privacy-preserving methods for sharing trajectories. Miranda-Pascual et al. [7] provide a detailed review of DP trajectory publishing approaches. Their work highlights the shortcomings of the existing approaches and motivates the need for further research. As one state-of-the-art representative for non-deep learning approaches, we include PrivTrace [16] (ref. Section 7.1), for its strong utility under DP and available source code. PrivTrace generates synthetic trajectories in three steps: 1) discretising the dataset's space with a density-aware grid, 2) training first- and second-order Markov models with DP, and 3) generating trajectories via a random walk algorithm.

As an alternative to traditional methods, Liu et al. [10] propose deep learning-based generative models for trajectory generation. Buchholz et al. [6] systematise SOTA deep generative models for trajectory data and introduce an evaluation framework. They show that these models offer strong utility but lack formal privacy guarantees. They also identify privacy risks in some models and recommend DP-SGD to mitigate them. However, DP-SGD requires models to avoid additional inputs during generation, unlike many SOTA models such as LSTM-TrajGAN [12]. Recently, diffusion models have emerged that do not rely on such inputs.

DiffTraj [11] is the first application of the Denoising Diffusion Probabilistic Model (DDPM) diffusion model for trajectory generation and serves as the baseline in this work. Its architecture is based on a UNet [33] with up- and downsampling modules built from ResNet blocks using Conv1D layers. An attention-based transition module [36] connects these components to capture sequential dependencies. The model supports optional *conditional information* for guided generation, such as average speed, distance, and start time. Despite these strengths, DiffTraj lacks formal privacy guarantees, and while diffusion models are more robust to MIA than GANs, they remain vulnerable [37].

Diff-RNTraj [17] generates trajectories directly on the road network, avoiding errors from generating GPS trajectories followed by map-matching. A spatial validity loss penalises unconnected segments, improving performance over baselines. However, it requires road network data and lacks formal privacy guarantees. We exclude Diff-RNTraj from our experiments due to these constraints.

To the best of our knowledge, ConvGAN [38] is the only approach applying DP-SGD to trajectory generation. While ConvGAN represents the first proof-of-concept for this methodology, the resulting model cannot generate trajectories with real-world utility, both with and without DP guarantees [38]. Therefore, we do not further consider ConvGAN.

5. Methodology

This section outlines the methodology to address the research questions defined in Section 1. As depicted in Figure 2, information flows from the real dataset D_{real} to the synthetic dataset D_{syn} along two paths. First, during training model parameters are updated using D_{train} (blue path). To ensure privacy w.r.t. the training data, we apply DP-SGD [35] (Section 5.1). Second, during generation (dotted path), the model optionally incorporates conditional information derived from D_{test}. To protect this input, we propose a novel DP conditional embedding mechanism (Section 5.2). The overall design aims to ensure formal guarantees along both paths and quantify the resulting utility-privacy trade-off. To generalise findings and assess the impact of model choice, we evaluate three generative model types – diffusion, GAN,

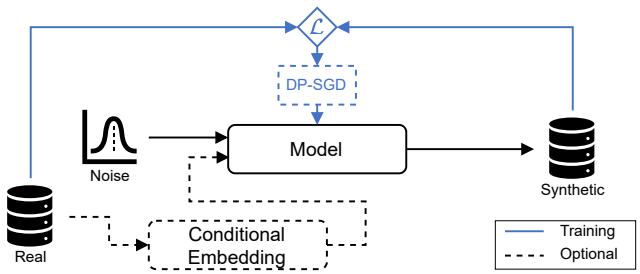

Figure 2. The dataset is connected to the synthetic data through two paths that leak information. First, during training, the model parameters are updated. Here, DP-SGD can ensure privacy. Second, conditional embedding is optionally derived from real samples and used during generation.

and VAE – detailed in Section 5.3. The privacy analysis of the proposed design is provided in Section 6.

5.1. Privacy of Training

During training, model parameters are updated using gradients derived from a loss. This loss reflects real data either directly, e.g., via the reconstruction loss in a VAE, or indirectly, e.g., via the discriminator in a GAN (ref. Section 2.3). Thus, model parameters may encode aspects of the real data necessary for generating realistic synthetic samples (ref. blue path in Figure 2). This risks memorising and reproducing training samples (via overfitting), and allows MIAs [39] to infer details about D_{train}. The most widely used method to prevent such leakage is DP-SGD[15, 35].

We use the Opacus library [40] with `PRV` accounting [41] to implement DP-SGD. The noise multiplier is predetermined based on the desired target values for $(\varepsilon_s, \delta_s)$, with $\varepsilon_s = 10.0$ as default. This value the largest value still considered offering realistic guarantees in DL [15]. Smaller values incur a high utility cost, while larger ones are too weak for formal guarantees [15], although they may still protect against specific attacks. We follow the standard recommendation $\delta_s = 1/n^{1.1}$ with $n = |D_{\text{train}}|$ [15].

DP-SGD is applied to all gradients for the diffusion model and VAE. For the GAN, only the generator is trained with DP, while the discriminator is trained without it to preserve training stability. This does not compromise privacy w.r.t. the synthetic data (or release of the generator), as the discriminator is not involved in generation. However, the discriminator must not be released.

5.2. Conditional Information

Most SOTA generative trajectory models, such as DiffTraj [11] and LSTM-TrajGAN [12], rely on conditional information for high utility. For instance, LSTM-TrajGAN uses encoded trajectories, while DiffTraj incorporates eight derived features. This creates an information flow from the real dataset D_{real} to the generated dataset D_{syn} (ref. ② in Figure 1). As a result, conditional models lack formal privacy guarantees, even when trained with DP-SGD. The risk of sensitive information leaking through conditional inputs has been demonstrated for LSTM-TrajGAN [6]. To mitigate

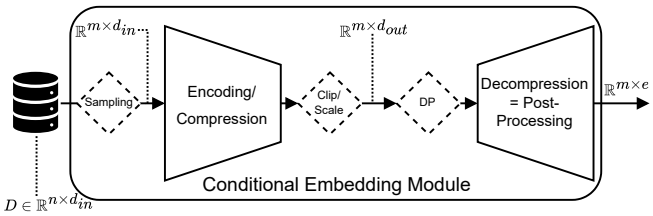

Figure 3. First, m samples from the dataset are selected uniformly at random. A neural network maps these samples to a lower-dimensional space d_{out}. Optionally, the per-sample norm is clipped/scaled, and a DP mechanism is applied. Finally, the resulting encoding is decompressed.

this risk, we introduce a novel DP conditional embedding mechanism that ensures privacy w.r.t. the cond. info. used during generation. It is illustrated in Figure 3 and marked by the black dotted box in Figure 2. We describe its components in the order they are applied.

1) Input Format. We consider two input formats of conditional information. The first format, referred to as ***8-Stat***, corresponds to the original DiffTraj [11] format and includes: 1) departure time, 2) total distance, 3) total duration, 4) total length, 5) average distance, 6) average speed, 7) start grid ID, 8) end grid ID. This input is embedded using the original wide-and-deep network [11]. If the DP mechanism is not enabled (threat models Ⓐ and Ⓑ), the resulting embedding is used directly and the following steps 2–6 are skipped.

The second format, ***Sample***, uses a full trajectory sample from the test set D_{test} as conditional input. Naturally, using a trajectory as conditional information suffers from the risk of the models returning the trajectory unaltered, as can happen with LSTM-TrajGAN [6]. Therefore, we never use this format without applying the DP mechanism, i.e., all steps 1–6 are mandatory.

2) Sampling. In the first step, we uniformly sample $m \leq |D_{test}|$ trajectories without replacement from D_{test}. This step is crucial for the privacy guarantees, and the value of m must be fixed upfront independently of the dataset to prevent information leakage.

3) Compression. The amount of noise added to achieve DP guarantees depends on the dimensionality of the data. Therefore, we compress the m samples to a lower-dimensional space d_{out} using a single Fully Connected (FC) layer.

4) Clipping and Scaling. To apply a DP mechanism, the sensitivity of each sample must be bounded (ref. Section 2.2). We achieve this by clipping or scaling the compressed embedding d to a fixed norm C. The norm type p depends on the DP mechanism used. For the Laplace ($p = 1$) and Gaussian ($p = 2$) mechanisms, we apply standard norm clipping as in DP-SGD [35]:

$$d_{\text{clipped}} = \min\left(1, \frac{C}{\|d\|_p}\right) \cdot d \tag{3}$$

For the VMF mechanism ($p = 2$), requiring values on the unit sphere, we instead rescale all vectors to norm C [42]: $d_{\text{scaled}} = \frac{C}{\|d\|_2} \cdot d$. Empirically, we observe that compression tends to fully utilise the available norm range. Therefore, we fix $C = 1.0$, which is compatible with all DP mechanisms.

5) DP Mechanism. We consider three DP mechanisms for the conditional embedding module: Laplace $\mathcal{L}$, Gaussian $\mathcal{N}$, and VMF $\mathcal{V}$. Unless stated otherwise, we use the Laplace mechanism, which performed best in preliminary experiments. The others variants are evaluated in ablation study III in Section 7.4.6. The Laplace and Gaussian mechanisms add i.i.d. noise to each component of the clipped embedding:

$$d_{\text{DP}} = d_{\text{clipped}} + \text{Noise}(\sigma) \tag{4}$$

with noise scale σ determined by the clipping norm C and privacy parameters ε_c (and δ_c for $\mathcal{N}$). The VMF mechanism replaces d_{scaled} with a unit vector sampled from the VMF distribution, using d_{scaled} as the mean direction and a concentration parameter κ. The values for σ and κ are detailed in the privacy analysis in Section 6.2.

Noise Schedule. During training, we apply a noise schedule similar to the β-schedule used in diffusion models [43]. For each sample in a batch, we draw a random value $\beta \sim \mathcal{U}(0, 1)$ and compute the final embedding as:

$$d_{\text{DP}} = \beta \cdot d_{\text{DP}} + (1 - \beta) \cdot d_{\text{clipped}}. \tag{5}$$

This approach allows the model to occasionally use less noisy embeddings, which helps stabilise training, while still adapting to the noise level used during generation. The noise schedule **must not** be applied during generation, as this would violate the privacy guarantees. However, since the training data is protected via DP-SGD, applying the schedule during training does not compromise privacy w.r.t. D_{train}.

6) Decompression. After the application of the DP mechanism, the noisy embedding d_{DP} is decompressed using one FC layer to the embedding dimension e used by the model. We fix $e = 512$ according to the value used by DiffTraj [11].

Summary. We consider six types of conditional embeddings:

1) **None:** Unconditional models.
2) **8-Stat:** Original DiffTraj [11] embedding.
3) **8-Stat + $\mathcal{L}$:** DiffTraj embedding with Laplace mechanism.
4) **Sample + $\mathcal{L}$:** Full sample with Laplace mechanism.
5) **Sample + $\mathcal{N}$:** Full sample with Gaussian mechanism.
6) **Sample + $\mathcal{V}$:** Full sample with VMF mechanism.

Sample encoding without DP is not considered, as this case does not provide any privacy and suffers the same risk as LSTM-TrajGAN [6]. The privacy guarantees of this conditional embedding module are proven in Section 6.2.

5.3. Model Architectures

We consider three generative model types: Diffusion, GAN, and VAE, each with an *unconditional* and *conditional* variant. The unconditional models follow standard structures (Section 2.3), while the conditional variants include the embedding module described in Section 5.2. Model architectures were kept similar to isolate the effect of model type.

Diffusion. As a diffusion model, we use the SOTA DiffTraj [11] model described in Section 4. The only difference is the addition of DP-SGD and the integration of the conditional embedding module outlined in the previous sections. The DiffTraj model is based on the UNet [33] architecture published by Rombach et al. [44, 45]. The proposed *Traj-UNet* consists of a downsampling and an upsampling module connected by a transition module. Both the down- and upsampling modules consist of multiple stacked ResNet blocks based on Conv1D layers. Moreover, each ResNet block receives the sum of the diffusion step's t embedding and the conditional embedding (if used) as secondary input. The downsampling blocks connect to the equivalent upsampling blocks through skip connections. The transition module uses an attention mechanism [36] between two ResNet blocks to capture sequential dependencies.

VAE. For the VAE, we split the Traj-UNet into two parts, using the UNetEncoder and UNetDecoder [44, 45]. The downsampling module represents the VAE's encoder, while the upsampling module represents the decoder. However, to enable both modules to capture sequential dependencies, we include the attention-based transition module both at the end of the encoder and the beginning of the decoder. As we split the Traj-UNet into two separate modules, no skip connections are used. Moreover, the ResNet blocks only receive the cond. info. as secondary input, the encoder returns the latent distribution parameters μ and σ (ref. Section 2.3), and the decoder applies a `tanh` activation to the output.

GAN. For the GAN, we initially tested using a full Traj-UNet for both generator and discriminator, but the increased complexity caused unstable training. Therefore, we used the UNetDecoder, also used by the VAE, as the generator and the UNetEncoder as the discriminator. Two layers, a Conv1D and a FC layer, were added to the discriminator to reduce the output to a single value. Using a full Traj-UNet in only one of the modules also yielded poor results due to imbalance. Since the standard adversarial loss caused unstable training, we used the WGAN-LP loss [46] for better stability, despite slower convergence. For non-DP-SGD training, we set $n_{\text{critic}} = 5$ to maintain a near-optimal discriminator, as $n_{\text{critic}} = 1$ performed poorly. In the evaluation, we report the total training steps, resulting in only 20 000 generator updates when using $n_{\text{critic}} = 5$. This setup ensures a runtime comparable to the diffusion model for the same total number of updates. Under DP-SGD, we set $n_{\text{critic}} = 1$ as the added noise sufficiently weakened the generator, making additional discriminator updates unnecessary. Thus, in this setting, generator updates equal the total steps.

6. Privacy Analysis

This section analyses the privacy guarantees of the proposed design. As outlined in Section 3, we assume that training and generation use disjoint datasets, i.e., $D_{\text{real}} = D_{\text{train}} \cup D_{\text{test}}$ and $D_{\text{train}} \cap D_{\text{test}} = \emptyset$. First, Section 6.1 examines the guarantees w.r.t. the training data D_{train} achieved through DP-SGD. Second, Section 6.2 analyses the guarantees w.r.t. the conditional information derived from D_{gen} during generation. Finally, Section 6.3 combines these individual guarantees to provide a comprehensive analysis of the privacy guarantees for the final synthetic dataset.

6.1. Privacy of Training

To provide formal guarantees w.r.t. the training data D_{train}, i.e., the blue path in Figure 2, we apply DP-SGD [35], as described in Section 5.1. We use the PRV [41] accounting method and denote the privacy parameters for DP-SGD as $(\varepsilon_s, \delta_s)$. Both threat models Ⓑ and Ⓓ (ref. Section 3) rely on DP-SGD to ensure privacy w.r.t. the training data.

Corollary 1. *All models trained with DP-SGD provide trajectory-level $(\varepsilon_s, \delta_s)$-differential privacy w.r.t. the training data D_{train} under the add-or-remove adjacency relation.*

As we use standard DP-SGD based on an established library, we refer to the proof of the privacy guarantees to Abadi et al. [35] and Gopi et al. [41]. Note that DP-SGD does not provide privacy guarantees w.r.t. the conditional information used during generation, which we address in the following.

6.2. Privacy Proof for Conditional Information

In the following, we derive the privacy guarantees w.r.t. the conditional information used as a secondary input for the generative model. These guarantees relate to the dotted path from the real data in Figure 2 and are relevant for threat models Ⓒ and Ⓓ. As outlined in Section 3, all guarantees are defined at the trajectory level, i.e., with respect to individual trajectories in the dataset. First, we formalise the per-sample compression function f_c (ref. Section 5.2):

Definition 2 (Per-Sample Compression Function)**.** *The per-sample compression function f_c maps an input sample $x \in \mathbb{R}^{d_{in}}$ to a lower-dimensional space $\mathbb{R}^{d_{out}}$, followed by norm clipping (or scaling for the VMF mechanism):*

$$f_c : \mathbb{R}^{d_{in}} \to \mathbb{R}^{d_{out}}, \quad x \mapsto f(x) \cdot \min\left\{\frac{C}{\|f(x)\|_p}, 1\right\} \quad (6)$$

where $f(x)$ is the output of a neural network, C is the norm bound, p the type of norm used, and d_{in} and d_{out} denote the input and output dimensions, respectively. Clipping ensures the output norm does not exceed C, while scaling (used for VMF) sets it exactly to C.

Here, samples represent trajectories, i.e., $x \in \mathbb{R}^{2\times L}$, where L denotes the sequence length. For simplicity, we flatten the sequence such that $d_{in} = 2L$. Note that the norm type p needs to be consistent throughout this proof, i.e., if the Laplace mechanism is used, $p = 1$ must hold for all equations, while $p = 2$ is required for the Gaussian and VMF mechanisms.

Next, we extend this function to a per-dataset function F_c. We consider a trajectory dataset $D = \{x_1, x_2, \ldots, x_n\}$, consisting of n samples from $\mathbb{R}^{d_{in}}$. As described in Section 5.2, we select $m < n$ samples uniformly at random without replacement from the dataset for generation, where m is a dataset-independent constant determined in advance.

Definition 3 (Dataset Compression Function)**.** *The dataset compression function F_c receives m samples and maps each sample independently to a lower-dimensional space $\mathbb{R}^{m\times d_{out}}$ using the per-sample function f_c:*

$$F_c : \mathbb{R}^{m\times d_{in}} \to \mathbb{R}^{m\times d_{out}}, D \mapsto \{f_c(x_i)\}_{i=1}^{m} \quad (7)$$

Each sample $x_i' = f_c(x_i)$ in the output only depends on the corresponding sample x_i in the input dataset, i.e., F_c represents a parallel composition of f_c over disjoint subsets of the dataset D.

We target trajectory-level privacy as the UoP and use the replace-one adjacency relation to define the neighbourhood of two datasets, i.e., one dataset is obtained from the other by replacing one sample with another. The common add-or-remove adjacency relation is not applicable here, as the output dimensionality of the compression function F_c depends on the number of input samples. Next, we define the privacy mechanism M_c^{Lap} based on the Laplace mechanism.

Definition 4 (Laplace Compression Mechanism with Subsampling)**.** *The compression mechanism M_c^{Lap} receives a dataset D, subsamples m samples uniformly at random without replacement, and adds independently drawn Laplace noise to all components of the output of the dataset compression function F_c:*

$$M_c^{Lap}(D) : \mathbb{R}^{n\times d_{in}} \to \mathbb{R}^{m\times d_{out}} D \mapsto F_c(D) + Y \quad (8)$$

where $Y \in \mathbb{R}^{m\times d_{out}}$ is a matrix with $Y_{ij} \sim Lap(\lambda)$.

Theorem 1 (Privacy of Laplace Compression Mechanism)**.** *The mechanism M_c^{Lap} provides $(\log(1 + \frac{m}{n}(e^{\varepsilon} - 1)), 0)$-DP w.r.t. the replace-one adjacency definition for $\lambda = \frac{2C}{\varepsilon}$ if $p = 1$.*

Proof. The result follows directly from the proof for the Laplace mechanism (ref. Theorem 3.6 in [23]). The value for λ corresponds to the sensitivity of the Laplace on replace-one adjacent datasets. Uniform subsampling without replacements provides amplification as per Theorem 9 in [47]. □

The Gaussian [23] or VMF [27] mechanisms can serve as a drop-in replacement for the Laplace mechanism. For these mechanisms, one must use the l_2-norm instead of the l_1-norm (i.e., $p = 2$), and additionally, the VMF requires fixing the norm bound $C = 1$ to obtain unit vectors. The Gaussian mechanism is useful when d_{out} is large, as the l_2-norm scales with $\sqrt{d_{out}}$ instead of d_{out}. The VMF mechanism has the advantage that only the direction of the conditional information vector changes, but not its norm, which might benefit some settings. We can define the Gaussian Compression Mechanism $M_c^{\mathcal{G}}$ as follows:

Definition 5 (Gaussian Compression Mechanism with Subsampling)**.** *The compression mechanism $M_c^{\mathcal{G}}$ receives a dataset D, subsamples m samples uniformly at random without replacement, and adds independently drawn Gaussian noise to all components of the output of F_c:*

$$M_c^{\mathcal{G}}(D) : \mathbb{R}^{n\times d_{in}} \to \mathbb{R}^{m\times d_{out}} D \mapsto F_c(D) + Z \quad (9)$$

where $Z \in \mathbb{R}^{m\times d_{out}}$ is a matrix with $Z_{ij} \sim \mathcal{N}(0, \sigma^2)$.

Theorem 2 (Privacy of Gaussian Compression Mechanism)**.** *For any $\varepsilon > 0$, $\delta \in (0,1)$, the compression mechanism $M_c^{\mathcal{G}}$ provides $(\log(1+\frac{m}{n}(e^{\varepsilon}-1)), \frac{m}{n}\delta)$-differential privacy w.r.t. the replace-one adjacency definition for $\sigma = \frac{\alpha 2C}{\sqrt{2\varepsilon}}$ if $p = 2$, where α is defined as per Algorithm 1 in [26].*

Proof. The theorem follows from the proof of the Analytical Gaussian mechanism (ref. Theorem 9 in [26]). Uniform subsampling without replacements provides amplification as per Theorem 9 in [47]. □

Finally, the VMF mechanism $M_c^{\mathcal{V}}$ can be defined as:

Definition 6 (VMF Compression Mechanism with Subsampling)**.** *The compression mechanism $M_c^{\mathcal{V}}$ receives a dataset D, subsamples m samples uniformly at random without replacement, and independently samples from a VMF distribution for each vector:*

$$M_c^{\mathcal{V}}(D) : \mathbb{R}^{n \times d_{in}} \to \mathbb{R}^{m \times d_{out}} D \mapsto \{\mathcal{V}(\kappa, F_c(D)_i)\}_{i=1}^{m} \tag{10}$$

where $\mathcal{V}(\kappa, x)$ denotes a sample from the VMF distribution with concentration parameter κ and mean direction x. Note that $C = 1$ as the VMF mechanism requires unit vectors.

Theorem 3 (Privacy of VMF Compression Mechanism)**.** *The mechanism $M_c^{\mathcal{V}}$ provides $(\log(1+\frac{m}{n}(e^{\varepsilon}-1)), 0)$-differential privacy w.r.t. the replace-one adjacency definition for $C = 1$ and $\kappa = \frac{\varepsilon}{2C} = \frac{\varepsilon}{2}$ if $p = 2$.*

Proof. This theorem follows from Corollary 2 in Faustini et al. [42], where the batches B and B' in the corollary correspond to our subsets of D and D', respectively, and uniform sampling without replacements provides amplification as per Theorem 9 in [47]. □

6.3. Combined Privacy Analysis

The training data D_{train} influences the generated dataset solely through its impact on the model parameters. Thus, whether conditional information used during training is protected by DP does not affect the privacy guarantees w.r.t. D_{train}. Accordingly, when using DP-SGD with privacy parameters ε_s and δ_s, the overall privacy for the training set is $(\varepsilon_s, \delta_s)$ under the add-or-remove adjacency relation. Without DP-SGD, no guarantees w.r.t. D_{train} are provided.

The privacy w.r.t. D_{test} is based on the privacy mechanism (Section 6.2) used during generation. Using a privacy mechanism during training does not influence the guarantees related to D_{test}. The generation process provides $(\varepsilon_c, \delta_c)$-DP w.r.t. the conditional information under the replace-one adjacency relation, if the DP conditional information mechanism is used. Unconditional models that do not use any input inherently provide $(0,0)$-DP w.r.t. conditional information, as the samples in D_{test} are never accessed.

Due to the differing adjacency relations, the privacy guarantees w.r.t. D_{train} and D_{test} cannot (trivially) be combined using the parallel composition theorem despite D_{train} and D_{test} being disjoint. We note that the replace-one adjacency relation is considered to be approx. twice as strong as the add-or-remove adjacency relation [15] (ref. Section 2.2). Thus, we evaluate the DP cond. info. mechanism for both $\varepsilon_c = 10$, and $\varepsilon_c = 20$, as the latter provides comparable privacy to DP-SGD with $\varepsilon_s = 10$.

Referring back to the threat model (Section 3): Setting Ⓐ provides no privacy guarantees, Ⓑ achieves $(\varepsilon_s, \delta_s)$-DP w.r.t. training data D_{train} under the add-or-remove adjacency relation, Ⓒ ensures $(\varepsilon_c, \delta_c)$-DP w.r.t. test set D_{test} under the replace-one adjacency relation, and Ⓓ provides both $(\varepsilon_s, \delta_s)$-DP w.r.t. training data under add-or-remove adjacency and $(\varepsilon_c, \delta_c)$-DP w.r.t. test set under replace-one adjacency. All guarantees are defined at the trajectory level, i.e., with respect to individual samples in the dataset, as outlined in Section 3.

7. Evaluation

In this section, we report the results of our experiments to address the research questions outlined in Section 1. First, we define the experimental setup in Section 7.1 and introduce the evaluation metrics in Section 7.2. Section 7.3 describes the used configurations, and Section 7.4 presents the results.

7.1. Experimental Setup

System Specifications. We performed the final experiments on a High-Performance Computing (HPC) cluster with notes having two Intel Xeon Platinum 8452Y CPUs (72 cores in total), 512 GB of RAM, running SUSE Linux Enterprise Server 15 SP4. For each experiment, we restricted the resources per node to one NVIDIA H100 NVL GPU (94 GB), 18 CPU cores, and 128 GB of RAM.

Datasets. Two real-world trajectory datasets are used for evaluation. Following the preprocessing steps of DiffTraj [11], both datasets are resampled to a fixed length and limited to a bounding box. The bounding box is chosen independent of the data based on geographical constraints, such as the fifth ring road for Beijing, to prevent privacy leakage. The first dataset is *Porto*[2] [19], containing GPS trajectories of taxis in Porto, Portugal. This dataset consists of 1 559 209 trajectories, resampled to a fixed length of 100 locations per trajectory. The second dataset is *Geolife*[3] [20], which includes GPS trajectories from 182 users. We use the preprocessed version provided in the artifacts of Buchholz et al. [6], containing 69 504 trajectories, resampled to a fixed length of 200 locations per trajectory.

Non-DL Baseline. As detailed in Section 4, we include PrivTrace [16] as a SOTA non-DL baseline. We use the authors' implementation[4] without modification. It uses hard-coded parameters K and κ that differ from those in the paper. As we received no response to our communication attempts and the formulas in [16] yield an intractable number of Markov states (i.e., the code does not terminate), we retain the implementation defaults. Since PrivTrace generates

2. $(lat_{min}, lon_{min}, lat_{max}, lon_{max}) = (41.10, -8.72, 41.24, -8.50)$
3. $(lat_{min}, lon_{min}, lat_{max}, lon_{max}) = (39.75, 116.19, 40.03, 116.56)$
4. https://github.com/DpTrace/PrivTrace

variable-length trajectories, we resample them to the fixed length of each dataset for a fair comparison.

Evaluation Process. First, we train each model variant on the respective training set. We split each dataset D into five folds such that each run uses a different fold for testing (D_{test}) and using $80\,\%$ of the dataset for training (D_{train}). Each configuration is repeated five times with different random seeds, and the results are averaged. The number of epochs is determined such that the number of steps is larger or equal to $100\,000$. After training, we generate $3\,000$ synthetic trajectories for each model and dataset and compare them to $3\,000$ real trajectories selected randomly from the respective test dataset D_{test}. If conditional information is used, the synthetic trajectories are matched with the real trajectories from which the conditional information was derived for the trajectory-level evaluation. Otherwise, we match the synthetic trajectories to the real trajectories using the Hungarian algorithm [48] and the average per-trajectory haversine distance [49] as the cost function.

7.2. Evaluation Metrics

The selection of evaluation metrics follows the guidelines of the framework proposed by Buchholz et al. [6], with parameters aligned to related work wherever possible. Implementation details are provided in the code repository[1]. Unless stated otherwise, distances are computed using the Haversine formula [49] and reported in metres.

To evaluate how well the generated data matches the overall *point distribution*, we use the *Sliced Wasserstein Distance (SWD)*. This metric compares the full 2D distribution of points directly, without requiring to discretise the data into a grid first. For comparability with existing methods [11], we also report (i) the *JSD* after discretising the space into a 64×64 grid, and (ii) the *Hausdorff Distance (HD)* between $100\,000$ randomly sampled real and synthetic points.

Point statistics evaluate how well local spatial patterns are preserved in the synthetic data. (i) *Range queries* [50] estimate local density by counting how many points lie within a radius r of a query location. We report the *Mean Relative Error (MRE)* over 200 random queries with radii $r \in \{50, 100, 200, 500, 1000\}\mathrm{m}$. (ii) *Hotspot analysis* [51] checks whether both datasets identify the same high-density regions. The space is divided into a $g \times g$ grid for $g = 128$, and cells exceeding the 95th percentile in density are marked as hotspots. The *Sørensen-Dice coefficient (SDC)* quantifies the overlap between real and synthetic hotspot sets.

At the *trajectory level*, we assess both preservation and statistical properties. (i) *Trajectory preservation* measures how closely synthetic trajectories replicate the shape and location of real ones. Reported metrics include the per-trajectory *HD*, the *normalised Haversine distance* (divided by trajectory length), and the *Dynamic Time Warping (DTW)*[52], which aligns points between two trajectories to minimise cumulative distance. (ii) *Trajectory statistics* describe global mobility behaviour, including the *Total Travelled Distance (TTD)*[53] (total length of a trajectory), the *trajectory diameter*[53] (maximum distance between any two points), and the *trip error* [53], which compares start-end patterns via transition probabilities between grid cells (using a $g \times g$ grid for $g = 16$). For the TTD and diameter, histograms are constructed using 55 bins (based on the rule of thumb $\sqrt{3000} \approx 55$) and compared using the *JSD*. The trip error is computed by flattening the transition matrices $U \in g^2 \times g^2$ and comparing them via *JSD*.

7.3. Configurations

To answer the three research questions, we vary the following parameters in our evaluation: I) First, we train each base configuration with and without DP-SGD to assess its impact across different settings. II) Second, we evaluate all six types of conditional information described in Section 5.2, namely: 1) no conditional information, 2) the DiffTraj embedding (8-Stat), 3) 8-Stat with Laplace noise ($\mathcal{L}$), 4) the proposed Sample embedding with Laplace noise ($\mathcal{L}$), 5) Gaussian noise ($\mathcal{N}$), and 6) VMF noise (VMF). III) Third, we test the three model architectures from Section 5.3 – DiffTraj, UNetVAE, and UNetGAN – to analyse the effect of the architecture on performance.

Unless stated otherwise, we use $\varepsilon_s = 10$ and $\delta = 1/n^{1.1}$ for DP-SGD, as reasoned in Section 5.1. The maximum gradient norm for DP-SGD is set to $C = 0.1$. For conditional information, we use $\varepsilon_c = 10$ and compute δ analogously based on the test set size. Since privacy amplification depends on the number of samples m, we conservatively assume $m = n$, i.e., the synthetic dataset matches the test set size. If fewer samples are generated (as in our evaluation), the actual guarantee is stronger than the reported ε_c due to amplification by subsampling. The dimensionality of compressed conditional information is fixed to $d_{out} = 8$.

Each configuration is identified by a unique ID. Configurations using DP cond. info. are repeated for $\varepsilon_c = 20$ and marked with an additional `a`, e.g., `5a` denotes the same setting as `5` but with a higher privacy budget for conditional information. We refer to IDs `1`–`24` as the *base configurations*, used to address the three main research questions. Additionally, we include three ablation studies (IDs `25`–`39`) to isolate specific parameter effects. The non-DL baseline PrivTrace is ID `40`. Due to high computational cost, ablation studies 2 and 3 are limited to the Porto dataset.

A preliminary hyperparameter search identified suitable learning rates, batch sizes, epochs, and clipping norms, aiming for consistency across configurations. A full search with formal tuning was not feasible due to resource constraints (ref. Section 7.4.7). A complete listing of all configurations is provided in Table 1 in the appendix.

7.4. Results

This section presents the evaluation results. Figures 5–10 show the SWD and JSD for Porto and GeoLife, respectively. Error bars indicate $95\,\%$ confidence intervals, threat models (ref. Section 3) are shown in the legends, and PrivTrace is abbreviated as `PT`. Confidence intervals are wide due to the

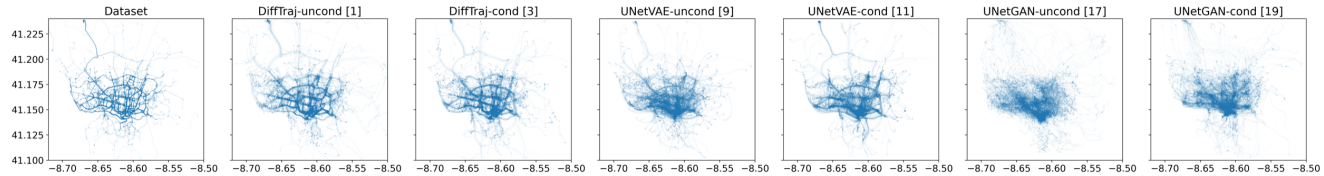

(a) Conditional models provide no formal guarantees (Ⓐ). Unconditional models provide formal guarantees w.r.t. the test data (Ⓒ).

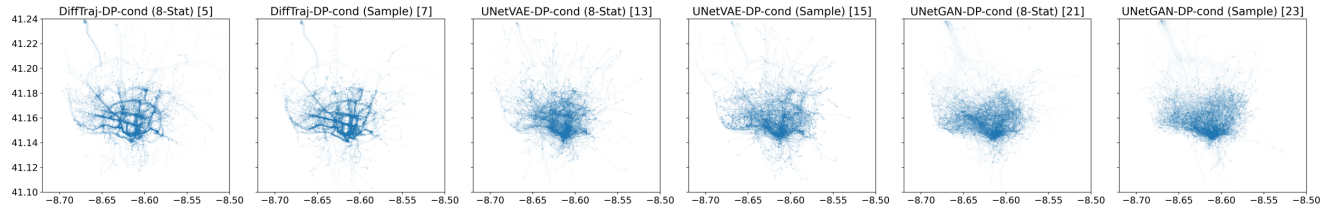

(b) All these models provide privacy guarantees w.r.t. the conditional information (Ⓒ).

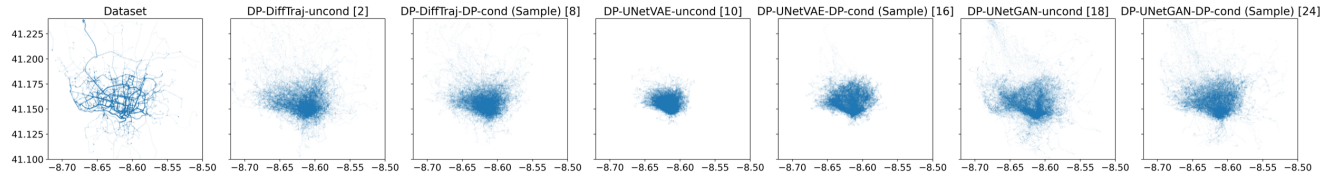

(c) All these models provide full formal guarantees (Ⓓ).

Figure 4. Example synthetic trajectories for Porto after ≈ 100 000 steps. The case IDs (ref. Table 1) are reported in brackets.

limited number of runs (five) per configuration. Additional runs were infeasible given the significant computational cost.

For our DP-cond. info. mechanism, we only show the Sample format with Laplace noise to simplify the plots, as the 8-Stat format yields similar results. Figure 4 shows the point distribution for 1 000 synthetic Porto trajectories. GeoLife examples are in the appendix (Figure 13). We focus our discussion on SWD and JSD, as these best reflect the observed distribution quality. Due to the large number of configurations and metrics, the remaining results are reported in the appendix in Table 2 and Table 3, respectively.

7.4.1. Research Question 1. Our first research question asked: *How does DP-SGD affect the generated trajectories' utility?* To answer this question, we trained each base configuration without (threat models Ⓐ and Ⓒ) and with DP-SGD (Ⓑ and Ⓓ) and compared the results. Figures 5, 6, 7, and 9 show non-DP-SGD cases in darker shades and DP-SGD cases in lighter shades of the same base colour. Comparing adjacent bars reveals that DP-SGD degrades performance across models except for UNetGAN, which performs similarly or even slightly better with DP-SGD.

On Porto, the SWD of the conditional DiffTraj (ID `3` vs `4`) and UNetVAE (ID `11` vs `12`) approximately doubles despite using conditional information without DP, and the unconditional VAE even increases its SWD by a factor of 8 (ID `9` vs `10`) (ref. Figure 5). The unconditional DiffTraj's SWD (ID `1` vs `2`) appears to be an outlier as it's the only DiffTraj measurement that does not show an increase when using DP-SGD. Moreover, this case's JSD increases 2.6-fold when using DP-SGD. This aligns with the example figures (Figure 4 and Figure 13) which show a substantial utility loss for all DiffTraj and UNetVAE models when using DP-SGD.

Interestingly, the UNetGAN performs similar (unconditional, ID `17` vs `18`) or even better (conditional, ID `19` vs `20`) with DP-SGD than without. This result is partly due to the poor performance of the non-DP model and the fact that DP-UNetGAN can update the generator more often, as it does not require increasing n_{critic} to 5 for stability. Nevertheless, the DP-UNetGAN outperforms the other models for threat models Ⓑ and Ⓓ regarding most point-level utility metrics

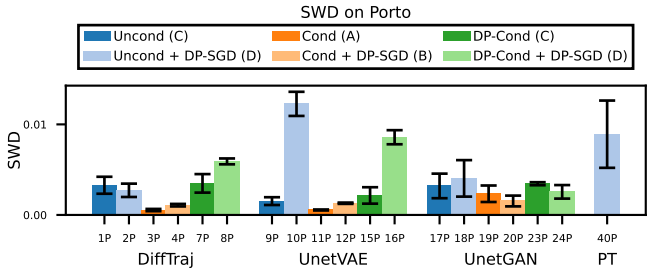

Figure 5. The bars depict the SWD for the Porto Taxi dataset.

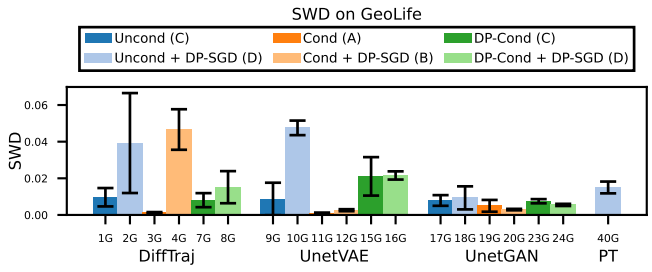

Figure 6. The bars depict the SWD for the GeoLife dataset.

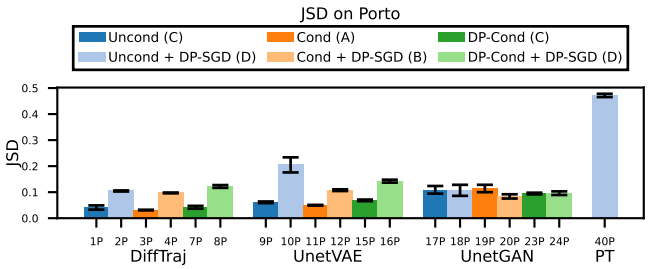

Figure 7. The bars depict the JSD for the Porto Taxi dataset.

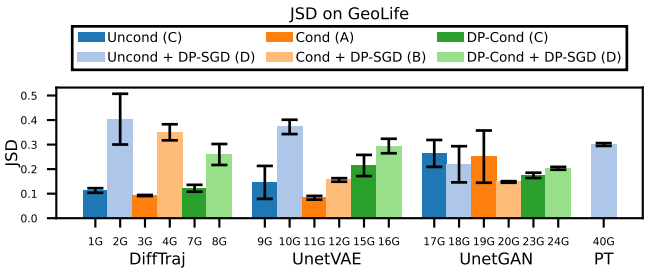

Figure 9. The bars depict the JSD for the GeoLife dataset.

on both datasets. This interesting finding might indicate that the best model in the standard setting (DiffTraj) does not necessarily translate to the best model under DP (UNetGAN).

Visually, Figures 4 and 13 show that synthetic data generated with DP-SGD retains the overall shape of the dataset but does not fully capture finer details, such as the road network. The DP version of unconditional DiffTraj (ID `2`) and both DP-UNetGAN variants (ID `18` and `24`) approximate the general distribution of the Porto dataset. Hence, these models may still be suitable for applications that require only coarse-grained density information.

In contrast, the GeoLife results are largely unusable (ref. Figure 13c). This can be attributed to the Porto dataset being over $20\times$ larger than GeoLife, as larger datasets generally yield better results under DP-SGD [15]. The bar plots for GeoLife (Figures 6 and 9) also show much larger confidence intervals than those for Porto (Figures 5 and 7), indicating less stable training and greater variability between runs.

Finally, while this paper focuses on deep learning models, we include PrivTrace as a SOTA non-deep learning baseline for comparison. When comparing the results to PrivTrace (ID `40`, labelled `PT` in the figures), most DP-SGD models outperform the baseline on Porto. On GeoLife, results are closer, but UNetGAN still surpasses PrivTrace. These findings show that deep learning models, despite being more recent, can achieve comparable utility to SOTA non-DL methods, underscoring their potential for trajectory generation. Still, future work is needed: in TM Ⓓ, neither the baseline nor the models provide sufficient utility for most downstream applications, as evident from the example figures 4 and 13.

Conclusion. To answer **RQ1**, our results show that DP-SGD incurs substantial utility loss in trajectory generation, restricting most applications. Nonetheless, performance remains comparable to non-DL baselines such as PrivTrace, underscoring the potential of deep learning models. Providing high utility using DP-SGD (Threat models Ⓑ and Ⓓ) is not feasible with the current state-of-the-art models and privacy mechanisms and requires further research.

7.4.2. Research Question 2. Second, we asked: *How can we use conditional information with differential privacy guarantees?* To answer this question, we proposed a method to provide formal guarantees w.r.t. the conditional information in Section 5.2. Here, we compare unconditional and conditional models using the DP cond. info. mechanism for DiffTraj and UNetGAN on Porto (Figure 8) and GeoLife (Figure 10), respectively. The left groups represent threat model Ⓒ (without DP-SGD), and the right groups represent threat model Ⓓ (with DP-SGD).

Without DP-SGD (TM Ⓒ), all three configurations of both model types perform similarly, revealing no benefit of using the DP cond. info. mechanism over an unconditional model. However, when applying DP-SGD (TM Ⓓ), the results become more interesting. For DiffTraj on Porto, the utility even degrades when using the DP cond. info. mechanism with either input format. However, for DiffTraj on GeoLife and for UNetGAN on both datasets, the DP cond. info. mechanism improves utility compared to the unconditional model. In these cases, the unconditional model performs worst, the 8-Stat format yields intermediate results, and the Sample format performs best.

For example, on Porto the UNetGAN using DP cond. info. with Sample format (ID `24`) represents the best model for threat model Ⓓ regarding all point-level metrics, and most on GeoLife. On GeoLife, the UNetGAN model exhibits noticeably improved point distributions when incorporating the DP cond. info. mechanism, both without (IDs `23` vs `17`) and with DP-SGD (IDs `24` vs `18`).

These results suggest that the DP cond. info. mechanism primarily enhances model stability. This is supported by two observations. First, UNetGAN benefits the most, consistent with GANs being notoriously unstable [54]. Second, the

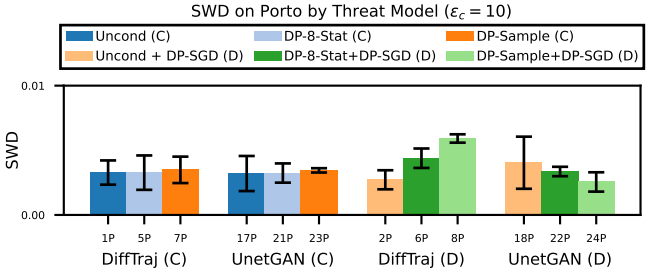

Figure 8. The bars depict the SWD ordered by threat model.

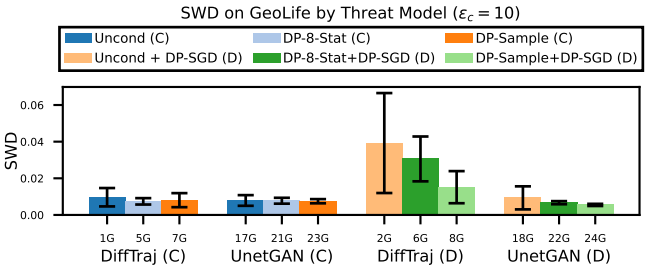

Figure 10. The bars depict the SWD ordered by threat model.

effect is stronger on the smaller GeoLife dataset, as smaller datasets generally lead to more unstable training.

Moreover, we note that the DP cond. info. mechanism becomes beneficial for TM Ⓒ when relaxing the privacy parameter to $\varepsilon_c = 20$. For example, without DP-SGD, DiffTraj with Sample DP cond. info. (ID 7a) reduces the SWD by 12 % on Porto and 30 % on GeoLife compared to the unconditional model (ID 1). While $\varepsilon_c = 20$ may seem weak, we highlight that the DP cond. info. mechanism is analysed w.r.t. the replace-one adjacency relation, which is considered approximately twice as strong as the common add-or-remove relation (ref. Section 6.3). Additionally, the ε_c values are computed under the worst-case assumption $m = n$, although we actually used $m = 3\,000 \ll n = D_{test}$ during evaluation. Accordingly, the true privacy level is higher than reported, and for sufficiently large datasets, the mechanism can yield benefits even under stricter guarantees.

Conclusion. To answer **RQ2**, our results show that the DP cond. info. mechanism generally improves utility when combined with DP-SGD (TM Ⓓ), especially for UNetGAN and on the smaller GeoLife dataset. Without DP-SGD (TM Ⓒ), it offers no clear benefit under stricter privacy settings but can yield improvements when relaxing ε_c. Overall, the mechanism enhances model stability and can improve utility, particularly for unstable models and smaller datasets.

7.4.3. Research Question 3. Finally, we asked: *Are certain model types better suited for formal privacy guarantees than others?* Without formal guarantees (TM Ⓐ), DiffTraj with conditional information (ID 3) yields the best metrics and visual results for Porto, confirming that diffusion models represent the current SOTA for trajectory generation. However, the conditional UNetVAE (ID 11) achieves similar results, even outperforming DiffTraj on several, mostly sequential, metrics. On Porto, the synthetic data produced by UNetVAE appears more blurry than that of DiffTraj (ref. Figure 4a). On GeoLife, the conditional UNetVAE (ID 11) outperforms DiffTraj (ID 3) on all but two metrics. This aligns with the general observation that diffusion models require larger datasets for optimal performance compared to VAE models (Porto contains 20 × more data than GeoLife). The UNetGAN (IDs 17 and 19) performs significantly worse than the other models for TM Ⓐ, both visually and based on the SWD metric (ref. Figure 5). The poorer performance may partly result from the reduced number of generator updates (ref. Section 5.3). However, increasing the updates by a factor of 5 (500 000 total), to match the other models, did not yield comparable results.

Furthermore, the results highlight the critical role of conditional information in improving the utility of synthetic data across all models. Visually, Figure 4a shows a clear difference between conditional and unconditional models. This is supported by the SWD values on Porto, which decrease by 84 % for DiffTraj (ID 1 vs 3), 64 % for UNetVAE (ID 9 vs 11), and 27 % for UNetGAN (ID 17 vs 19) when conditional information is used. This trend is also evident in the corresponding bar plots Figure 5 and Figure 6.

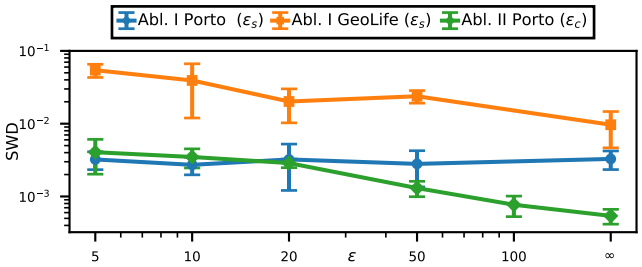

Figure 11. Ablation studies I and II with 95 % conf. Intervals over log-scale. ∞ indicates configurations without DP.

We already discussed the different models in the context of DP-SGD in Section 7.4.1. UNetGAN achieves the best performance under DP-SGD on both datasets, followed by the diffusion model, while UNetVAE performs consistently poorly in all cases involving DP-SGD. These findings indicate that the model with the best non-DP performance is not necessarily optimal when privacy guarantees are required. The reasons for this behaviour remain unclear. The GAN may benefit from DP-SGD being applied only to the generator, which has roughly half the parameters of the other models (ref. Section 5.3). This results in less relative noise per gradient update, which may explain the improved performance.

Conclusion. Without DP-SGD, the diffusion model DiffTraj achieves the best performance, followed closely by the UNetVAE. However, when applying DP-SGD, the UNetGAN outperforms both other models, indicating that the best model in the non-DP setting is not necessarily optimal under DP.

7.4.4. Ablation Study I: Influence of ε_s. In our first ablation study (Figure 11), we varied the privacy parameter $\varepsilon_s \in \{5, 10, 20, 50\}$ of DP-SGD for the unconditional DiffTraj. On GeoLife, we observe the expected trend: increasing ε_s improves utility, as indicated by the decreasing SWD (orange curve in Figure 11). Even at $\varepsilon_s = 50$, the model performs significantly worse than without DP-SGD, with an SWD that is 2.5 × higher than the non-DP model (ID 1 vs 27). On Porto (blue curve), we do not observe a clear correlation between ε_s and SWD. However, other metrics such as JSD confirm the expected trend, with the largest JSD of 0.108 for $\varepsilon_s = 5$ (ID 25) and the smallest JSD of 0.040 9 for the non-DP model (ID 1). Hence, the SWD results on Porto appear to be an outlier.

7.4.5. Ablation Study II: Influence of ε_c. Similarly, we varied the privacy parameter $\varepsilon_c \in \{5, 10, 20, 50, 100\}$ for the conditional DiffTraj model with DP cond. info. of Sample format (green curve in Figure 11). The figure shows a clear correlation between increasing ε_c and decreasing SWD. While $\varepsilon_c = 50$ (ID 30) yields a 140 % increase in SWD compared to the non-DP model (ID 3), $\varepsilon_c = 100$ (ID 31) reduces the gap to 42 %.

7.4.6. Ablation Study III: DP Mechanisms. As the third ablation study, we compared the three DP cond. info. mechanisms – Laplace, Gaussian, and VMF– introduced in

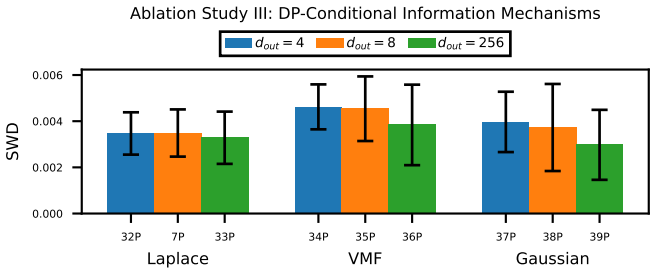

Figure 12. Ablation Study III. Each group represents one of the three DP cond. info. mechanisms, and the colours indicate the d_{out} value.

Section 5.2, using $d_{out} \in \{4, 8, 256\}$ and $\varepsilon_c = 10$. Figure 12 depicts the SWD results for the Porto dataset. For fixed ε_c, all mechanisms perform similarly. The only configuration that clearly outperforms the default Laplace mechanism with $d_{out} = 8$ (ID 7) is the Gaussian mechanism with $d_{out} = 256$ (ID 39). However, this mechanism performs better only regarding point-based metrics, while degrading most sequential metrics. For $d_{out} \in \{4, 8\}$, the Laplace mechanism remains the best choice, followed by the Gaussian mechanism. Despite the dependency on the l_1-norm, which suggested worse performance for larger d_{out}, the Laplace mechanism performs consistently across all d_{out} values. In contrast, the Gaussian mechanism performs well only at $d_{out} = 256$. The VMF mechanism yields the poorest results among the three mechanisms. While the mechanism improves with larger d_{out}, this comes at the cost of significantly increased runtime (ref. Section 7.4.7). In conclusion, choosing between the Laplace mechanism at small d_{out} and the Gaussian mechanism at large d_{out} appears most promising. The VMF mechanism does not appear suitable for this task.

7.4.7. Runtimes. All runtimes are based on the hardware specified in Section 7.1 and reported in Table 1 for Porto. Geolife runtimes are slightly higher due to the increased trajectory length. DiffTraj trains the longest, e.g., $\approx 6\,\mathrm{h}$ for the conditional baseline, while the VAE and GAN require $\approx 2\,\mathrm{h}$ and $\approx 5\,\mathrm{h}$, respectively. Matching the number of generator updates in UNetGAN to those of the other models increases the training time to $\approx 25\,\mathrm{h}$, which justifies our choice to align total training steps instead. Unconditional models generally train significantly faster than their conditional counterparts, with minimal differences for VAE.

Using DP-SGD increases runtimes by a factor of 5–10. For instance, the conditional DiffTraj requires $\approx 54\,\mathrm{h}$ (ID 4), VAE $\approx 29\,\mathrm{h}$, and GAN $\approx 32\,\mathrm{h}$. The smaller relative increase for UNetGAN is due to only the generator being trained with DP-SGD such that the discriminator, thereby half of the total parameters, is updated without DP-SGD.

The DP cond. info. mechanism has negligible runtime impact. Only the VMF mechanism incurs significant overhead for large d_{out}, but this configuration is impractical due to poor performance (ref. Section 7.4.6). Notably, PrivTrace runtimes are significantly higher than reported in [16] due to hard-coded parameters K and κ (ref. Section 7.1), which result in a larger amount of Markov states.

For all cases, evaluation took approximately $9\,\mathrm{min}$, with most of the time spent on metric computation. Generating $3\,000$ samples took $< 1\,\mathrm{s}$ for the VAE and GAN, and $\approx 20\,\mathrm{s}$ for the diffusion model. Generation is unaffected by DP-SGD, as it applies only during training.

8. Discussion

Some authors suggest that the inherent obfuscation of the generative process alone suffices to protect privacy [11]. However, this method does not provide formal privacy guarantees [6]. MIA [34] can recover training data from a model, and an overfitted model may leak private information. We acknowledge that recovering private information from synthetic data is challenging, and such obfuscation may suffice in low-risk scenarios. However, using cond. info. during generation introduces a more significant risk. For example, Buchholz et al. [6] showed that LSTM-TrajGAN can reproduce trajectories nearly identical to its inputs.

Guarantees w.r.t. generation inputs D_{test} (TM Ⓒ) are attainable today with moderate utility loss, e.g., using unconditional DiffTraj (ID 1) or DiffTraj with DP cond. info. (ID 5 or 7). In contrast, protecting both training and test data (TM Ⓓ) leads to severe utility loss, rendering most models unsuitable for real-world applications, as clearly visible in Figure 4. Still, the utility for this threat model Ⓓ remains comparable to SOTA non-DL baselines such as PrivTrace. This highlights the potential of deep learning models, and future work on differentially private deep learning may render them viable for privacy-preserving data generation in high-risk settings in the future.

Meanwhile, a hybrid approach can be considered for models with generation-time inputs, such as conditional models. Here, DP-SGD is omitted, i.e., no guarantees are provided w.r.t. D_{train}, but the cond. info. (D_{test}) is protected via mechanisms such as the proposed DP cond. info. mechanism or utilising unconditional models. Although lacking formal guarantees towards the full dataset, this method can constitute a reasonable compromise in specific contexts, especially when combined with diffusion models, which show reduced susceptibility to MIAs (but remain vulnerable [37]). Mitigating direct links between generation inputs and outputs can reduce risks and direct leakage, such as those demonstrated in [6].

Limitations. Despite careful hyperparameter selection and preliminary testing, the high computational cost limited the number of configurations we could evaluate. Therefore, we cannot guarantee that the optimal configuration or each model was found but are confident that the tested configurations offer a representative performance overview and reveal valid trends. Although the final utility depends on factors such as available resources, dataset properties, and the use case, the results serve as a solid starting point for model selection.

9. Conclusion

In this work, we set out to answer the question: *What is the (utility) cost of formal privacy guarantees for deep*

learning-based trajectory generation? To this end, we evaluated the utility of synthetic trajectory data using three model types – VAE, GAN, and diffusion models – with and without DP-SGD and conditional information. The evaluation covered two real-world datasets and eleven metrics. In total, we analysed over 90 configurations to examine the effect of various parameters on the utility-privacy trade-off.

The results revealed several key findings. First, DP-SGD significantly reduces the utility of generated trajectories. While acceptable utility may still be achievable for specific use cases with sufficiently large datasets, full formal privacy guarantees remain restrictive for most practical applications. Nonetheless, comparison to a SOTA non-DL baseline, PrivTrace, shows that deep learning models can achieve comparable or better utility under DP, underscoring their potential for trajectory generation. Second, we proposed a novel DP mechanism to enable the use of conditional information with formal DP guarantees w.r.t. the real data and formally proved its guarantees. Although the DP cond. info. mechanism does not consistently outperform unconditional models, it improves training stability especially combined with DP-SGD, for unstable models, and on smaller datasets. Third, the comparison of model types confirmed that, without formal privacy guarantees, diffusion models generally offer the best performance. However, the evaluated VAE performed strongly on smaller datasets. Under DP-SGD, the GAN exhibited superior performance, demonstrating that the best model without privacy does not necessarily remain optimal when guarantees are applied. All source code has been made available to support future research.

Acknowledgements

The authors would like to thank UNSW, the Commonwealth of Australia, and the Cybersecurity Cooperative Research Centre Limited for their support of this work.

References

[1] V. Primault, A. Boutet, S. B. Mokhtar, and L. Brunie, "The Long Road to Computational Location Privacy: A Survey," *IEEE Commun. Surveys Tuts.*, vol. 21, no. 3, pp. 2772–2793, 2019. doi:10.1109/COMST.2018.2873950

[2] Y.-A. de Montjoye, C. A. Hidalgo, M. Verleysen, and V. D. Blondel, "Unique in the Crowd: The Privacy Bounds of Human Mobility," *Sci. Rep.*, vol. 3, no. 1, pp. 1–5, Dec. 2013. doi:10.1038/srep01376

[3] L. Franceschi-Bicchierai, "Redditor Cracks Anonymous Data Trove to Pinpoint Muslim Cab Drivers," 2015. Available: https://mashable.com/archive/redditor-muslim-cab-drivers (Accessed 2021-09-28).

[4] H. Jiang, J. Li, P. Zhao, F. Zeng, Z. Xiao, and A. Iyengar, "Location Privacy-Preserving Mechanisms in Location-Based Services: A Comprehensive Survey," *ACM Comput. Surv.*, vol. 54, no. 1, pp. 4:1–4:36, Jan. 2021. doi:10.1145/3423165

[5] À. Miranda-Pascual, P. Guerra-Balboa, J. Parra-Arnau, J. Forné, and T. Strufe, "An Overview of Proposals towards the Privacy-Preserving Publication of Trajectory Data," *Int. J. Inf. Secur.*, vol. 23, Sep. 2024. doi:10.1007/s10207-024-00894-0

[6] E. Buchholz, A. Abuadbba, S. Wang, S. Nepal, and S. S. Kanhere, "SoK: Can Trajectory Generation Combine Privacy and Utility?" *PoPETS*, vol. 2024, no. 3, pp. 75–93, Jul. 2024. doi:10.56553/popets-2024-0068

[7] À. Miranda-Pascual, P. Guerra-Balboa, J. Parra-Arnau, J. Forné, and T. Strufe, "SoK: Differentially Private Publication of Trajectory Data," *Proc. Priv. Enhancing Technol. (PoPETs)*, vol. 2023, pp. 496–516, 2023. doi:10.56553/popets-2023-0065

[8] E. Buchholz, A. Abuadbba, S. Wang, S. Nepal, and S. S. Kanhere, "Reconstruction Attack on Differential Private Trajectory Protection Mechanisms," in *Proc. 38th Annu. Comput. Secur. Appl. Conf.* New York, NY, USA: ACM, Dec. 2022, pp. 279–292. doi:10.1145/3564625.3564628

[9] M. Shao, J. Li, Q. Yan, F. Chen, H. Huang, and X. Chen, "Structured Sparsity Model Based Trajectory Tracking Using Private Location Data Release," *IEEE Trans. Depend. Sec. Comput.*, vol. 18, no. 6, pp. 2983–2995, 2020. doi:10.1109/TDSC.2020.2972334

[10] X. Liu, H. Z. Chen, and C. Andris, "Trajgans: Using Generative Adversarial Networks for Geo-Privacy Protection of Trajectory Data (Vision Paper)," in *Workshop LoPaS*. Melbourne, Australia: github.io, 2018, pp. 1–7. Available: https://ptal-io.github.io/lopas2018/papers/LoPaS2018_Liu.pdf

[11] Y. Zhu, Y. Ye, S. Zhang, X. Zhao, and J. J. Q. Yu, "DiffTraj: Generating GPS Trajectory with Diffusion Probabilistic Model," in *Adv. Neural Inf. Process. Syst.*, ser. 1, vol. 23. New Orleans, USA: Curran Associates, Inc., 2023, p. 21. doi:10.5555/3666122.3668965

[12] J. Rao, S. Gao, Y. Kang, and Q. Huang, "LSTM-TrajGAN: A Deep Learning Approach to Trajectory Privacy Protection," *Leibniz Int. Proc. Inform.*, vol. 177, no. GIScience, pp. 1–16, 2020. doi:10.4230/LIPIcs.GIScience.2021.I.12

[13] A. Kapp, J. Hansmeyer, and H. Mihaljević, "Generative Models for Synthetic Urban Mobility Data: A Systematic Literature Review," *ACM Comput. Surv.*, vol. 56, no. 4, pp. 1–37, Apr. 2024. doi:10.1145/3610224

[14] F. Jin, W. Hua, M. Francia, P. Chao, M. Orlowska, and X. Zhou, "A Survey and Experimental Study on Privacy-Preserving Trajectory Data Publishing," *IEEE Trans. Knowl. Data Eng.*, vol. 35, no. 6, 2023. doi:10.1109/TKDE.2022.3174204

[15] N. Ponomareva, S. Vassilvitskii, Z. Xu, B. McMahan, A. Kurakin, and C. Zhang, "How to DP-fy ML: A Practical Guide to Machine Learning with Differential Privacy," in *Proc. 29th ACM SIGKDD Conf. Knowl. Discov. Data Min.*, ser. Kdd '23. New York, NY, USA: ACM, 2023, pp. 5823–5824. doi:10.1145/3580305.3599561

[16] H. Wang, Z. Zhang, T. Wang, S. He, M. Backes, J. Chen, and Y. Zhang, "PrivTrace: Differentially Private Trajectory Synthesis by Adaptive Markov Models," in *32nd USENIX Security Symposium*. Anaheim, CA,

USA: USENIX Association, 2023, pp. 1649–1666. doi:10.48550/arXiv.2210.00581

[17] T. Wei, Y. Lin, S. Guo, Y. Lin, Y. Huang, C. Xiang, Y. Bai, and H. Wan, "Diff-RNTraj: A Structure-Aware Diffusion Model for Road Network-Constrained Trajectory Generation," *IEEE Trans. Knowl. Data Eng.*, vol. 36, no. 12, pp. 7940–7953, 2024. doi:10.1109/TKDE.2024.3460051

[18] Z. Tao, W. Xu, and X. You, "Map2Traj: Street Map Piloted Zero-Shot Trajectory Generation with Diffusion Model," *arXiv*, no. arXiv:2407.19765, Jul. 2024. doi:10.48550/arXiv.2407.19765

[19] L. Moreira-Matias, M. Ferreira, J. Mendes-Moreira, L. L., and J. J., "Porto Taxi - Taxi Service Trajectory - Prediction Challenge, ECML PKDD 2015," 2015. doi:10.24432/C55W25

[20] Y. Zheng, L. Zhang, X. Xie, and W.-Y. Ma, "Mining Interesting Locations and Travel Sequences from GPS Trajectories," in *Proc. 18th Int. Conf. World Wide Web*, ser. WWW '09. New York, NY, USA: ACM, Apr. 2009, pp. 791–800. doi:10.1145/1526709.1526816

[21] Z. Tu, K. Zhao, F. Xu, Y. Li, L. Su, and D. Jin, "Protecting Trajectory from Semantic Attack Considering K-Anonymity, l-Diversity, and t-Closeness," *IEEE TNSM*, vol. 16, no. 1, pp. 264–278, Mar. 2019. doi:10.1109/TNSM.2018.2877790

[22] A. Majeed and S. O. Hwang, "Rectification of Syntactic and Semantic Privacy Mechanisms," *IEEE Security Privacy*, vol. 21, no. 5, pp. 18–32, Sep. 2023. doi:10.1109/MSEC.2022.3188365

[23] C. Dwork and A. Roth, "The Algorithmic Foundations of Differential Privacy," *Found. Trends Theor. Comput. Sci.*, vol. 9, no. 3-4, pp. 211–407, 2013. doi:10.1561/0400000042

[24] P. Guerra-Balboa, A. M. Pascual, J. Parra-Arnau, J. Forne, and T. Strufe, "Anonymizing Trajectory Data: Limitations and Opportunities," in *Third AAAI Workshop Priv.-Preserv. Artif. Intell. PPAI-22*, vol. 28. Virtual: PPAI, 2022, p. 10. doi:10.5445/IR/1000148633

[25] Ú. Erlingsson, V. Pihur, and A. Korolova, "RAPPOR: Randomized Aggregatable Privacy-Preserving Ordinal Response," in *Proc. 2014 ACM SIGSAC CCS*. New York, USA: ACM, Nov. 2014, pp. 1054–1067. doi:10.1145/2660267.2660348

[26] B. Balle and Y.-X. Wang, "Improving the Gaussian Mechanism for Differential Privacy: Analytical Calibration and Optimal Denoising," in *Proc. 35th Int. Conf. Mach. Learn.*, ser. Proceedings of Machine Learning Research, J. Dy and A. Krause, Eds., vol. 80. Stockholm, Sweden: PMLR, Jul. 2018, pp. 394–403. doi:10.48550/arXiv.1805.06530

[27] B. Weggenmann and F. Kerschbaum, "Differential Privacy for Directional Data," in *Proc. 2021 ACM SIGSAC CCS*. Virtual Event Republic of Korea: ACM, Nov. 2021, pp. 1205–1222. doi:10.1145/3460120.3484734

[28] P. Eigenschink, T. Reutterer, S. Vamosi, R. Vamosi, C. Sun, and K. Kalcher, "Deep Generative Models for Synthetic Sequential Data: A Survey," *IEEE Access*, vol. 11, pp. 47 304–47 320, 2023. doi:10.1109/ACCESS.2023.3275134

[29] D. Bank, N. Koenigstein, and R. Giryes, "Autoencoders," *arXiv*, no. arXiv:2003.05991, Apr. 2021. doi:10.48550/arXiv.2003.05991

[30] D. P. Kingma and M. Welling, "Auto-Encoding Variational Bayes," *arXiv*, no. arXiv:1312.6114, 2013. doi:10.48550/arXiv.1312.6114

[31] I. J. Goodfellow, J. Pouget-Abadie, M. Mirza, B. Xu, D. Warde-Farley, S. Ozair, A. Courville, and Y. Bengio, "Generative Adversarial Networks," *Commun. ACM*, vol. 63, no. 11, pp. 139–144, 2014. doi:10.1145/3422622

[32] J. Ho, A. Jain, and P. Abbeel, "Denoising Diffusion Probabilistic Models," *arXiv*, no. arXiv:2006.11239, Dec. 2020. doi:10.48550/arXiv.2006.11239

[33] O. Ronneberger, P. Fischer, and T. Brox, "U-Net: Convolutional Networks for Biomedical Image Segmentation," *arXiv*, no. arXiv:1505.04597, May 2015. doi:10.48550/arXiv.1505.04597

[34] R. Shokri, M. Stronati, C. Song, and V. Shmatikov, "Membership Inference Attacks against Machine Learning Models," in *2017 IEEE Symp. Secur. Priv. SP*. San Jose, CA, USA: IEEE, May 2017, pp. 3–18. doi:10.1109/SP.2017.41

[35] M. Abadi, A. Chu, I. Goodfellow, H. B. McMahan, I. Mironov, K. Talwar, and L. Zhang, "Deep Learning with Differential Privacy," in *Proc. 2016 ACM SIGSAC CCS*. New York, NY, USA: ACM, 2016, pp. 308–318. doi:10.1145/2976749.2978318

[36] A. Vaswani, N. Shazeer, N. Parmar, J. Uszkoreit, L. Jones, A. N. Gomez, L. Kaiser, and I. Polosukhin, "Attention Is All You Need," *arXiv*, no. arXiv:1706.03762, Aug. 2023. doi:10.48550/arXiv.1706.03762

[37] T. Matsumoto, T. Miura, and N. Yanai, "Membership Inference Attacks against Diffusion Models," in *2023 IEEE Secur. Priv. Workshop SPW*. San Francisco, CA, USA: IEEE, May 2023, pp. 77–83. doi:10.1109/SPW59333.2023.00013

[38] J. Merhi, E. Buchholz, and S. S. Kanhere, "Synthetic Trajectory Generation through Convolutional Neural Networks," in *2024 21st Annu. Int. Conf. Priv. Secur. Trust PST*, ser. PST'24, vol. 21. Sydney, NSW, Australia: IEEE, Aug. 2024, pp. 1–12. doi:10.1109/PST62714.2024.10788061

[39] R. Shokri, G. Theodorakopoulos, G. Danezis, J.-P. Hubaux, and J.-Y. Le Boudec, "Quantifying Location Privacy: The Case of Sporadic Location Exposure," in *Lecture Notes in Computer Science*. Berlin, Heidelberg: Springer, 2011, vol. 6794 LNCS, pp. 57–76. doi:10.1007/978-3-642-22263-4_4

[40] A. Yousefpour *et al.*, "Opacus: User-Friendly Differential Privacy Library in PyTorch," *arXiv*, no. arXiv:2109.12298, Sep. 2021. doi:10.48550/arXiv.2109.12298

[41] S. Gopi, Y. T. Lee, and L. Wutschitz, "Numerical Composition of Differential Privacy," in *Adv. Neural Inf.*

Process. Syst., M. Ranzato, A. Beygelzimer, Y. Dauphin, P. Liang, and J. W. Vaughan, Eds., vol. 34. Online: Curran Associates, Inc., 2021, pp. 11 631–11 642. doi:10.5555/3540261.3541150

[42] P. Faustini, N. Fernandes, S. Tonni, A. McIver, and M. Dras, "Directional Privacy for Deep Learning," *arXiv*, no. arXiv:2211.04686, 2022. doi:10.48550/arXiv.2211.04686

[43] P. Dhariwal and A. Nichol, "Diffusion Models Beat GANs on Image Synthesis," in *Adv. Neural Inf. Process. Syst.*, M. Ranzato, A. Beygelzimer, Y. Dauphin, P. Liang, and J. W. Vaughan, Eds., vol. 34. Online: Curran Associates, Inc., 2021, pp. 8780–8794. doi:10.5555/3540261.3540933

[44] Robin Rombach, A. Blattmann, D. Lorenz, P. Esser, and B. Ommer, "High-Resolution Image Synthesis with Latent Diffusion Models," in *2022 IEEECVF Conf. Comput. Vis. Pattern Recognit. CVPR*. New Orleans, LA, USA: IEEE, Jun. 2022, pp. 10 674–10 685. doi:10.1109/CVPR52688.2022.01042

[45] R. Rombach, A. Blattmann, D. Lorenz, P. Esser, and B. Ommer, "CompVis/Latent-Diffusion," CompVis LMU Munich, Sep. 2024. Available: https://github.com/CompVis/latent-diffusion (Accessed 2024-09-26).

[46] H. Petzka, A. Fischer, and D. Lukovnicov, "On the Regularization of Wasserstein GANs," in *Int. Conf. Learn. Represent.*, vol. 6. Vancouver, BC, Canada: ICLR, Mar. 2018, p. 24. doi:10.48550/arXiv.1709.08894

[47] B. Balle, G. Barthe, and M. Gaboardi, "Privacy Amplification by Subsampling: Tight Analyses via Couplings and Divergences," in *Adv. Neural Inf. Process. Syst.*, S. Bengio, H. Wallach, H. Larochelle, K. Grauman, N. Cesa-Bianchi, and R. Garnett, Eds., vol. 31. Montreal, QC, Canada: Curran Associates, Inc., 2018, p. 11. doi:10.5555/3327345.3327525

[48] H. W. Kuhn, "The Hungarian Method for the Assignment Problem," *Nav. Res. Logist. (NRL)*, vol. 52, no. 1, pp. 7–21, Feb. 2005. doi:10.1002/nav.20053

[49] C. C. Robusto, "The Cosine-Haversine Formula," *Am. Math. Mon.*, vol. 64, no. 1, pp. 38–40, 1957. doi:10.2307/2309088

[50] R. Chen, B. C. M. Fung, and B. C. Desai, "Differentially Private Trajectory Data Publication," *arXiv*, no. arXiv:1112.2020, Dec. 2011. doi:10.48550/arXiv.1112.2020

[51] T. Cunningham, K. Klemmer, H. Wen, and H. Ferhatosmanoglu, "GeoPointGAN: Synthetic Spatial Data with Local Label Differential Privacy," May 2022. doi:10.48550/arXiv.2205.08886

[52] M. Müller, "Dynamic Time Warping," in *Information Retrieval for Music and Motion*. Berlin, Heidelberg: Springer, 2007, pp. 69–84. doi:10.1007/978-3-540-74048-3_4

[53] X. Sun, Q. Ye, H. Hu, Y. Wang, K. Huang, T. Wo, and J. Xu, "Synthesizing Realistic Trajectory Data with Differential Privacy," *IEEE Trans. Intell. Transp. Syst.*, vol. 24, no. 5, pp. 5502–5515, May 2023. doi:10.1109/TITS.2023.3241290

[54] M. Arjovsky, S. Chintala, and L. Bottou, "Wasserstein Generative Adversarial Networks," in *Proc. 34th Int. Conf. Mach. Learn.*, ser. Proceedings of Machine Learning Research, D. Precup and Y. W. Teh, Eds., vol. 70. PMLR, Aug. 2017, pp. 214–223. doi:10.48550/arXiv.1701.07875

[55] Damien Desfontaines, "The Privacy Loss Random Variable," Mar. 2020. Available: https://desfontain.es/blog/privacy-loss-random-variable.html (Accessed 2024-06-17).

Appendix A. All Results

In the following we provide detailed information on the used configurations (Table 1), the results of the evaluation (Table 2 and Table 3), and examples of synthetic trajectories for the second dataset GeoLife (Figure 13).

Appendix B. Symbols

Adj Adjacency
C Norm Bound
$D_{\textbf{real}}$ Real Dataset
$D_{\textbf{syn}}$ Synthetic Dataset
$D_{\textbf{test}}$ Test Dataset. Dataset during Generation.
$D_{\textbf{train}}$ Training Dataset
L Trajectory Length
δ_c Failure probability (imprecise but commonly used term [55]) used for cond. info.
δ_s Failure probability (imprecise but commonly used term [55]) used in DP-SGD
$\mathbb{R}$ Real Numbers
$\mathcal{K}$ Privacy Mechanism
$\mathcal{L}(\lambda)$ Laplace Distribution with scale λ
$\mathcal{N}(\mu, \sigma^2)$ Normal (Gaussian) Distribution with mean μ and variance σ^2
$\mathcal{U}(a, b)$ Uniform Distribution with bounds a and b
$\mathcal{V}(\kappa, \mu)$ Von Mises-Fisher Distribution with mean μ and concentration κ
$\mathbb{P}$ Probability
ε_c Privacy loss parameter used for conditional information
ε_s Privacy loss parameter used in DP-SGD
$\|\cdot\|_1$ l_1-Norm (Manhattan Norm)
$\|\cdot\|_2$ l_2-Norm (Euclidean Norm)
$\|\cdot\|_p$ l_p-Norm
d_{in} Input Dimension
d_{out} Output Dimension
f_c Sample Compression Function
n Number of Samples in the Dataset
p Type of Norm. $p = 1$ for l_1-Norm, $p = 2$ for l_2-Norm

Appendix C. Abbreviations

AdamW Pytorch's Adamw Optimizer with Decoupled Weight Decay

AE Autoencoder
Conv1D 1D Convolution
DDPM Denoising Diffusion Probabilistic Model
DL Deep Learning
DP Differential Privacy
DP-SGD Differentially Private Stochastic Gradient Descent
DTW Dynamic Time Warping
FC Fully Connected layer. Also called *Dense* (TensorFlow) or *Linear* (PyTorch) layer
GAN Generative Adversarial Network
HD Hausdorff Distance
HPC High-Performance Computing
i.i.d. independent and identically distributed random variables
JSD Jensen Shannon Divergence
MIA Membership Interference Attack
MRE Mean Relative Error
PDF Probability Density Function
SDC Sørensen-Dice coefficient
SOTA State Of The Art
SWD Sliced Wasserstein Distance
TM Threat Model
TTD Total Travelled Distance
UoP Unit of Privacy
VAE Variational Autoencoder
VMF Von Mises-Fisher Distribution
w.r.t. with respect to
WGAN-LP WGAN with Lipschitz Penalty [46]

TABLE 1. OVERVIEW OF ALL EVALUATION CONFIGURATIONS. THE TABLE LISTS THE VARIABLE PARAMETERS OF ALL TEST CASES. REFER TO SECTION 7.3 FOR AN EXPLANATION OF THESE VALUES. THE RESULTS FOR ALL CASES ARE LISTED IN TABLE 2 AND TABLE 3. THE MEAN RUNTIMES ARE REPORTED FOR THE PORTO DATASET. RUNTIMES ON THE GEOLIFE DATASET ARE SLIGHTLY HIGHER DUE TO THE INCREASED TRAJECTORY LENGTH.

ID	Model	DP-SGD	ε_s	Cond. Info.	Cond. DP.	ε_c	d_{out}	TM	Runtime
DiffTraj									
1	DiffTraj	✗	–	None	–	–	–	Ⓒ	03:04:58h
2	DiffTraj	✓	10.0	None	–	–	–	Ⓓ	27:59:13h
3	DiffTraj	✗	–	8-Stat	None	–	–	Ⓐ	05:55:18h
4	DiffTraj	✓	10.0	8-Stat	None	–	–	Ⓑ	53:25:46h
5*(a)*	DiffTraj	✗	–	8-Stat	$\mathcal{L}$	10.0 / *20.0*	8	Ⓒ	05:58:09h
6*(a)*	DiffTraj	✓	10.0	8-Stat	$\mathcal{L}$	10.0 / *20.0*	8	Ⓓ	53:26:53h
7*(a)*	DiffTraj	✗	–	Sample	$\mathcal{L}$	10.0 / *20.0*	8	Ⓒ	05:54:40h
8*(a)*	DiffTraj	✓	10.0	Sample	$\mathcal{L}$	10.0 / *20.0*	8	Ⓓ	52:09:51h
UNetVAE									
9	UNetVAE	✗	–	None	–	–	–	Ⓒ	02:08:03h
10	UNetVAE	✓	10.0	None	–	–	–	Ⓓ	28:38:35h
11	UNetVAE	✗	–	8-Stat	None	–	–	Ⓐ	02:17:50h
12	UNetVAE	✓	10.0	8-Stat	None	–	–	Ⓑ	33:01:06h
13*(a)*	UNetVAE	✗	–	8-Stat	$\mathcal{L}$	10.0 / *20.0*	8	Ⓒ	02:20:26h
14*(a)*	UNetVAE	✓	10.0	8-Stat	$\mathcal{L}$	10.0 / *20.0*	8	Ⓓ	33:40:07h
15*(a)*	UNetVAE	✗	–	Sample	$\mathcal{L}$	10.0 / *20.0*	8	Ⓒ	02:18:22h
16*(a)*	UNetVAE	✓	10.0	Sample	$\mathcal{L}$	10.0 / *20.0*	8	Ⓓ	31:49:42h
UNetGAN									
17	UNetGAN	✗	–	None	–	–	–	Ⓒ	04:41:02h
18	UNetGAN	✓	10.0	None	–	–	–	Ⓓ	28:40:34h
19	UNetGAN	✗	–	8-Stat	None	–	–	Ⓐ	05:03:54h
20	UNetGAN	✓	10.0	8-Stat	None	–	–	Ⓑ	31:28:14h
21*(a)*	UNetGAN	✗	–	8-Stat	$\mathcal{L}$	10.0 / *20.0*	8	Ⓒ	05:06:41h
22*(a)*	UNetGAN	✓	10.0	8-Stat	$\mathcal{L}$	10.0 / *20.0*	8	Ⓓ	31:43:34h
23*(a)*	UNetGAN	✗	–	Sample	$\mathcal{L}$	10.0 / *20.0*	8	Ⓒ	05:01:23h
24*(a)*	UNetGAN	✓	10.0	Sample	$\mathcal{L}$	10.0 / *20.0*	8	Ⓓ	30:53:21h
Ablation Study I: Varying ε_s									
25	DiffTraj	✓	5.0	None	–	–	–	Ⓓ	27:54:51h
2	DiffTraj	✓	10.0	None	–	–	–	Ⓓ	27:59:13h
26	DiffTraj	✓	20.0	None	–	–	–	Ⓓ	28:11:25h
27	DiffTraj	✓	50.0	None	–	–	–	Ⓓ	28:19:53h
Ablation Study II: Varying ε_c									
28	DiffTraj	✗	–	Sample	$\mathcal{L}$	5.0	8	Ⓒ	05:53:38h
7	DiffTraj	✗	–	Sample	$\mathcal{L}$	10.0	8	Ⓒ	05:54:40h
29	DiffTraj	✗	–	Sample	$\mathcal{L}$	20.0	8	Ⓒ	05:54:31h
30	DiffTraj	✗	–	Sample	$\mathcal{L}$	50.0	8	Ⓒ	05:52:39h
31	DiffTraj	✗	–	Sample	$\mathcal{L}$	100.0	8	Ⓒ	05:54:18h
Ablation Study III: Varying DP-Conditional Information Mechanisms									
32	DiffTraj	✗	–	Sample	$\mathcal{L}$	10.0	4	Ⓒ	05:53:47h
7	DiffTraj	✗	–	Sample	$\mathcal{L}$	10.0	8	Ⓒ	05:54:40h
33	DiffTraj	✗	–	Sample	$\mathcal{L}$	10.0	256	Ⓒ	06:01:03h
34	DiffTraj	✗	–	Sample	$\mathcal{V}$	10.0	4	Ⓒ	06:08:50h
35	DiffTraj	✗	–	Sample	$\mathcal{V}$	10.0	8	Ⓒ	06:07:07h
36	DiffTraj	✗	–	Sample	$\mathcal{V}$	10.0	256	Ⓒ	13:36:42h
37	DiffTraj	✗	–	Sample	$\mathcal{N}$	10.0	4	Ⓒ	05:54:44h
38	DiffTraj	✗	–	Sample	$\mathcal{N}$	10.0	8	Ⓒ	05:55:41h
39	DiffTraj	✗	–	Sample	$\mathcal{N}$	10.0	256	Ⓒ	05:57:36h
Non-Deep Learning Baseline: PrivTrace									
40	PrivTrace	–	10.0	–	–	–	–	Ⓓ	93:36:17h

TABLE 2. THIS TABLE LISTS THE METRIC RESULTS FOR ALL PORTO CASES. REFER TO TABLE 1 FOR THE CONFIGURATION OF EACH CASE. THE BEST BASELINE CASE (1–24) FOR EACH THREAT MODEL IS HIGHLIGHTED IN A SPECIFIC COLOUR. THE (A) CASES USE $\varepsilon_c = 20$ AND ARE NOT CONSIDERED FOR THE COMPUTATION OF THESE BEST VALUES. HOWEVER, IF ONE OF THE (A) CASES BEATS THE RESPECTIVE BEST CASE THE VALUE IS BOLDED.

ID	TM	JSD (↓)	SWD (↓)	HD (P) (↓)	Range (↓)	Hotspot (↑)	HD (T) (↓)	Haversine (↓)	DTW (↓)	TTD (↓)	TD (↓)	TE (↓)
DiffTraj												
1P	C	0.0409	0.00328	2124	0.111	0.896	1198	665	5.42e+04	0.0171	0.0143	0.216
2P	D	0.105	0.00272	3133	0.151	0.833	1255	713	6.37e+04	0.156	0.0349	0.298
3P	A	0.0313	0.000541	1617	0.0575	0.958	867	741	5.17e+04	0.047	0.00461	0.154
4P	B	0.097	0.00108	2320	0.135	0.865	1252	977	8.1e+04	0.223	0.0153	0.257
5P	C	0.041	0.00327	2684	0.0992	0.914	2745	2119	2.04e+05	0.0603	0.0237	0.211
6P	D	0.116	0.00439	4101	0.157	0.825	2542	1922	1.85e+05	0.0183	0.0276	0.294
7P	C	0.0419	0.00349	2475	0.101	0.912	2773	1924	1.84e+05	0.0147	0.0135	0.208
8P	D	0.122	0.00591	4528	0.162	0.832	2325	1644	1.58e+05	0.0168	0.0285	0.286
5aP	C	**0.0382**	0.00222	2401	**0.0869**	0.919	2167	1675	1.55e+05	0.0437	0.0212	0.211
6aP	D	0.111	0.00352	4174	0.155	0.831	2165	1617	1.52e+05	0.0255	0.0276	0.286
7aP	C	0.041	0.00287	2700	**0.0957**	0.921	2052	1349	1.24e+05	0.0179	0.0144	**0.204**
8aP	D	0.106	0.00391	4511	0.15	**0.842**	1678	1132	1.02e+05	0.0236	0.0207	0.269
UNetVAE												
9P	C	0.0611	0.00153	2395	0.1	0.921	1029	552	4.66e+04	0.0199	0.0157	0.231
10P	D	0.205	0.0123	7458	0.221	0.825	2169	1326	1.25e+05	0.0362	0.0312	0.326
11P	A	0.0498	0.000548	1319	0.066	0.922	782	656	4.56e+04	0.0261	0.0107	0.149
12P	B	0.108	0.00129	2048	0.106	0.842	897	682	5.29e+04	0.0408	0.0166	0.201
13P	C	0.0686	0.00287	2923	0.118	0.892	3584	2853	2.81e+05	0.0196	0.0128	0.234
14P	D	0.15	0.00812	6922	0.2	0.805	2625	2052	2.01e+05	0.0322	0.028	0.297
15P	C	0.0685	0.00215	2802	0.109	0.894	3906	2912	2.87e+05	0.0209	0.0125	0.236
16P	D	0.142	0.00858	7022	0.205	0.827	2499	1760	1.73e+05	0.0579	0.0284	0.315
13aP	C	0.0669	0.00291	2319	0.113	0.906	3052	2350	2.28e+05	0.0197	0.0151	0.23
14aP	D	0.12	0.00541	6689	0.18	0.817	2039	1688	1.63e+05	0.033	0.0287	0.297
15aP	C	0.069	0.0028	2439	0.115	0.9	2877	2035	1.99e+05	0.019	0.0186	0.236
16aP	D	0.107	0.00573	6387	0.176	**0.851**	2025	1440	1.4e+05	0.0299	0.0233	0.295
UNetGAN												
17P	C	0.109	0.0032	2634	0.157	0.802	1350	796	6.97e+04	0.0174	0.0194	0.327
18P	D	0.107	0.00404	2285	0.161	0.822	1270	774	6.69e+04	0.0224	0.0179	0.282
19P	A	0.114	0.00234	2060	0.141	0.817	1110	892	6.98e+04	0.0286	0.0141	0.276
20P	B	0.0837	0.00154	1725	0.101	0.867	935	783	5.87e+04	0.0343	0.0107	0.199
21P	C	0.0887	0.00324	3831	0.132	0.863	2564	1873	1.78e+05	0.0243	0.0144	0.254
22P	D	0.102	0.00336	3483	0.147	0.83	2862	2121	2.04e+05	0.0249	0.0154	0.276
23P	C	0.0948	0.00345	4242	0.148	0.855	2557	1788	1.71e+05	0.0172	0.0143	0.252
24P	D	0.096	0.00255	2005	0.134	0.84	2701	1874	1.79e+05	0.0218	0.0185	0.268
21aP	C	0.0868	0.00296	4060	0.13	0.87	2147	1557	1.44e+05	0.0248	0.0163	0.263
22aP	D	**0.0866**	**0.00179**	2386	**0.122**	**0.848**	2120	1556	1.43e+05	0.0295	0.0163	**0.253**
23aP	C	0.088	**0.00147**	2879	0.123	0.855	2025	1364	1.26e+05	0.0209	0.0176	0.255
24aP	D	**0.09**	**0.00138**	2164	**0.127**	**0.853**	2097	1410	1.3e+05	0.0221	0.0182	0.272
Ablation Study I: Varying ε_s												
25P	D	0.108	0.00323	3279	0.16	0.832	1290	742	6.63e+04	0.173	0.0348	0.303
2P	D	0.105	0.00272	3133	0.151	0.833	1255	713	6.37e+04	0.156	0.0349	0.298
26P	D	0.104	0.00323	2975	0.157	0.828	1280	736	6.54e+04	0.114	0.028	0.295
27P	D	0.1	0.0028	2785	0.146	0.83	1238	702	6.26e+04	0.0579	0.0256	0.286
Ablation Study II: Varying ε_c												
28P	C	0.0475	0.00406	2588	0.104	0.871	3509	2545	2.49e+05	0.0133	0.00927	0.217
7P	C	0.0419	0.00349	2475	0.101	0.912	2773	1924	1.84e+05	0.0147	0.0135	0.208
29P	C	0.041	0.00287	2700	0.0957	0.921	2052	1349	1.24e+05	0.0179	0.0144	0.204
30P	C	0.0357	0.0013	2544	0.0766	0.943	1182	725	5.87e+04	0.0176	0.0141	0.188
31P	C	0.0313	0.00077	2117	0.0649	0.964	769	456	3.33e+04	0.0204	0.0133	0.169
Ablation Study III: Varying DP-Conditional Information Mechanisms												
32P	C	0.0444	0.00347	2789	0.103	0.894	2788	1951	1.87e+05	0.149	0.0342	0.209
7P	C	0.0419	0.00349	2475	0.101	0.912	2773	1924	1.84e+05	0.0147	0.0135	0.208
33P	C	0.0437	0.00328	2814	0.102	0.89	2882	2026	1.95e+05	0.029	0.0143	0.208
34P	C	0.0505	0.00462	2492	0.12	0.888	2925	2085	2.02e+05	0.152	0.0342	0.216
35P	C	0.0515	0.00454	2638	0.116	0.89	3312	2374	2.32e+05	0.0154	0.0201	0.216
36P	C	0.0454	0.00384	2071	0.108	0.892	4073	3085	3.06e+05	0.0296	0.0129	0.212
37P	C	0.0456	0.00397	3869	0.109	0.889	3855	2884	2.85e+05	0.277	0.0492	0.21
38P	C	0.0464	0.00373	2337	0.108	0.873	3973	2956	2.92e+05	0.13	0.0149	0.209
39P	C	0.0406	0.00298	2362	0.0999	0.913	4100	3084	3.05e+05	0.0454	0.0126	0.206
Non-Deep Learning Baseline: PrivTrace												
40P	D	0.472	0.00892	5015	0.247	0.671	2562	1451	1.42e+05	0.25	0.538	0.534

TABLE 3. THIS TABLE LISTS THE METRIC RESULTS FOR ALL GEOLIFE CASES. REFER TO TABLE 1 FOR THE CONFIGURATION OF EACH CASE. THE BEST BASELINE CASE (1–24) FOR EACH THREAT MODEL IS HIGHLIGHTED IN A SPECIFIC COLOUR. THE (A) CASES USE $\varepsilon_c = 20$ AND ARE NOT CONSIDERED FOR THE COMPUTATION OF THESE BEST VALUES. HOWEVER, IF ONE OF THE (A) CASES BEATS THE RESPECTIVE BEST CASE THE VALUE IS BOLDED.

ID	TM	JSD (↓)	SWD (↓)	HD (P) (↓)	Range (↓)	Hotspot (↑)	HD (T) (↓)	Haversine (↓)	DTW (↓)	TTD (↓)	TD (↓)	TE (↓)
DiffTraj												
1G	C	**0.113**	0.00967	5755	**0.115**	**0.826**	1655	1192	2.31e+05	0.104	**0.00788**	**0.139**
2G	D	0.404	0.0392	8167	0.435	0.262	5797	5159	1.03e+06	**0.103**	0.205	0.408
3G	A	0.0924	0.00116	3376	0.0877	**0.907**	871	777	1.41e+05	0.089	0.00826	0.0962
4G	B	0.35	0.0466	6416	0.345	0.484	1e+04	8887	1.78e+06	0.0327	0.202	0.414
5G	C	0.13	**0.00743**	6179	0.131	0.794	4775	4151	8.28e+05	0.172	0.0104	0.157
6G	D	0.34	0.0306	6729	0.338	0.401	9170	8188	1.64e+06	0.299	0.394	0.434
7G	C	0.122	0.00807	6062	0.119	0.804	4224	3565	7.12e+05	0.164	0.0105	0.142
8G	D	0.26	0.0152	**5349**	0.24	0.565	5319	4348	8.68e+05	0.243	0.321	0.336
5aG	C	0.143	0.00867	6412	0.145	0.789	3741	3250	6.47e+05	0.154	0.0109	0.163
6aG	D	0.321	0.026	6786	0.328	0.437	7711	6705	1.34e+06	0.267	0.394	0.424
7aG	C	0.126	**0.00677**	6467	**0.113**	**0.84**	2889	2312	4.6e+05	0.0892	0.00883	0.139
8aG	D	0.237	0.0104	5379	0.198	0.594	3643	2719	5.41e+05	0.212	0.334	0.33
UNetVAE												
9G	C	0.146	0.00872	8643	0.129	0.779	**1601**	**1147**	**2.23e+05**	**0.0374**	0.0203	0.176
10G	D	0.372	0.0475	2.38e+04	0.181	0.564	5322	4738	9.47e+05	0.44	0.278	0.363
11G	A	**0.0833**	**0.00105**	3802	**0.0837**	0.903	**802**	**695**	**1.25e+05**	**0.00998**	**0.00706**	**0.091**
12G	B	0.156	**0.00258**	**5253**	0.121	**0.841**	**1451**	1068	2.1e+05	0.0382	**0.07**	**0.168**
13G	C	0.183	0.0153	1.15e+04	0.163	0.661	5482	4881	9.76e+05	0.0523	0.0207	0.197
14G	D	0.266	0.0327	2.04e+04	0.217	0.575	5323	4636	9.26e+05	0.352	0.232	0.291
15G	C	0.215	0.0211	1.35e+04	0.159	0.672	5053	4495	8.99e+05	0.12	0.0353	0.218
16G	D	0.294	0.0216	2.07e+04	0.241	0.537	4546	3907	7.8e+05	0.335	0.287	0.301
13aG	C	0.17	0.0124	1.21e+04	0.158	0.728	3128	2611	5.22e+05	0.0844	0.0321	0.173
14aG	D	0.225	0.0207	1.79e+04	0.231	0.574	3934	3287	6.55e+05	0.346	0.245	0.267
15aG	C	0.176	0.0128	1.23e+04	0.152	0.708	2848	2321	4.64e+05	0.129	0.0377	0.182
16aG	D	0.222	0.0139	1.59e+04	0.193	0.668	3379	2691	5.36e+05	0.334	0.286	0.249
UNetGAN												
17G	C	0.264	0.0079	**5169**	0.193	0.66	2075	1311	2.55e+05	0.0801	0.1	0.277
18G	D	0.22	0.00932	8201	**0.168**	**0.702**	**1937**	**1297**	**2.56e+05**	0.194	0.229	**0.193**
19G	A	0.251	0.00498	**3282**	0.168	0.744	1408	1108	2.07e+05	0.0588	0.0715	0.234
20G	B	**0.148**	0.00293	7158	**0.118**	0.839	1459	**1056**	**2.03e+05**	**0.0239**	0.126	0.169
21G	C	0.172	0.00776	8399	0.152	0.752	4154	3492	6.97e+05	0.0842	0.0942	0.215
22G	D	**0.193**	0.00669	1.08e+04	0.176	0.688	4149	3546	7.08e+05	0.171	**0.194**	0.207
23G	C	0.175	0.00749	8038	0.162	0.774	4129	3352	6.69e+05	0.118	0.0848	0.222
24G	D	0.203	**0.00547**	8987	0.176	0.695	4063	3480	6.95e+05	0.173	0.212	0.203
21aG	C	0.181	**0.00682**	9029	0.163	0.74	3212	2628	5.24e+05	0.135	0.113	0.214
22aG	D	**0.176**	**0.00533**	1.05e+04	**0.159**	**0.746**	2932	2341	4.67e+05	0.178	0.226	0.2
23aG	C	0.165	**0.00366**	**5113**	0.14	0.818	3047	2398	4.76e+05	0.0798	0.0603	0.193
24aG	D	0.195	**0.00509**	9157	0.168	**0.742**	2860	2279	4.54e+05	0.193	0.226	0.201
Ablation Study I: Varying ε_s												
25G	D	0.432	0.0543	5823	0.46	0.08	7875	6774	1.35e+06	0.121	0.278	0.482
2G	D	0.404	0.0392	8167	0.435	0.262	5797	5159	1.03e+06	0.103	0.205	0.408
26G	D	0.289	0.0202	7129	0.244	0.571	3135	2577	5.14e+05	0.0543	0.187	0.278
27G	D	0.263	0.0238	6766	0.196	0.635	3244	2757	5.5e+05	0.135	0.0831	0.239
Non-Deep Learning Baseline: PrivTrace												
40G	D	0.3	0.015	1.11e+04	0.167	0.793	2211	1671	3.32e+05	0.155	0.323	0.169

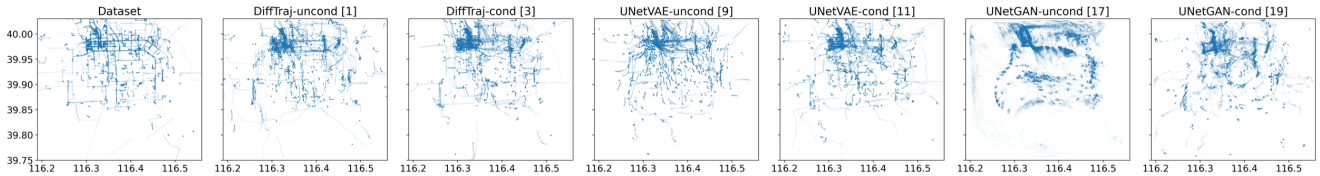

(a) Conditional models provide no formal guarantees (Ⓐ). Unconditional models provide formal guarantees w.r.t. the test data (Ⓒ).

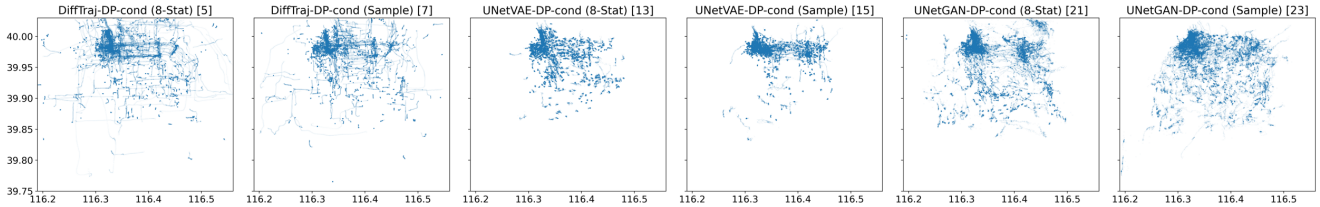

(b) All these models provide privacy guarantees w.r.t. the conditional information (Ⓒ).

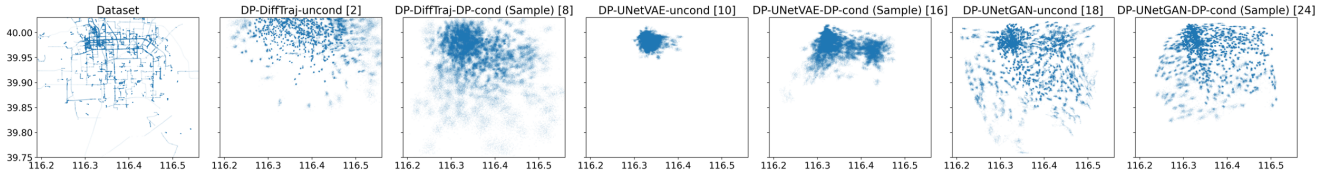

(c) All these models provide full formal guarantees (Ⓓ).

Figure 13. Example synthetic trajectories for GeoLife after $\approx 100\,000$ steps. The case IDs (ref. Table 1) are reported in brackets.